ABSTRACT

GANAPATHY, ANIRUDH RAMNATH. Evaluation of a Multi-Metal Approach to Iontophoretic Antibacterial Prophylaxis and Treatment in Orthopaedic Implants. (Under the direction of Dr. Rohan A. Shirwaiker.)

Rapid advances in medicine and developments in technology, combined with a growing population of senior citizens have precipitated a sharp rise in the dependence of healthcare on implantable medical devices. Although these devices drastically improve the patient's quality of life, serious concerns exist due to the risk of infection caused at the site of implantation. These infections are difficult to diagnose and treat, causing additional suffering and a huge financial burden on patients and the healthcare system. The rampant use of antibiotics to prevent such infections has led to the evolution of antibiotic-resistant "superbugs" like Methicillin-resistant *Staphylococcus aureus* (MRSA), which lays emphasis on the need for a non-antibiotic based method of preventing or treating orthopaedic infections.

Silver has been used since ancient times to treat wounds and burns to prevent infection. Many commercially available silver-based dressings and topically applied creams exploit the release of bactericidal Ag^+ ions in aqueous solutions. However, the release of Ag^+ ions is difficult to regulate in this form, and this is a cause for concern as silver is cytotoxic and overexposure to silver has adverse health effects.

Prior research developed a system by which Ag^+ ions could be iontophoretically released from silver electrodes using low-intensity direct currents (LIDC) in order to kill bacterial cells. This offered a method by which the release of Ag^+ ions could be controlled, as governed by Faraday's Law of Electrolysis. By applying this principle in orthopaedic implants, an antibacterial system was developed. However, due to the cytotoxic effects of silver, there exists a need to minimize the quantity of silver used in such a system.

The proposed research is aimed at minimizing the quantity of silver in an iontophoretic antibacterial orthopaedic implant device by partially substituting the cathodes with less toxic materials, without compromising the antibacterial efficacy of the system. The objectives of this research are as follows:

- Develop and evaluate an alternative multi-metal configuration of an iontophoretic LIDC activated antibacterial system for orthopaedic implants by using different electrode material combinations (Anode-Cathode configurations: Silver-Titanium and Silver-Stainless Steel), and compare their effectiveness with the prior design (Anode-Cathode Configuration: Silver-Silver)

- Assess the effects of two design parameters – cathode surface area and electrode separation distance – on the antibacterial efficacy of the system which uses dissimilar metals as electrodes.

The results suggest that the substitution of cathode materials with Titanium and Stainless Steel in the iontophoretic antibacterial system does not compromise its antibacterial efficacy. These metals are less cytotoxic, more biocompatible and more economical materials than silver. The design of the iontophoretic antibacterial orthopaedic implant device can be optimized as titanium and stainless steel may serve a dual purpose as both cathodic materials as well as structural materials. Furthermore, the results suggest that the antibacterial efficacy of the system is independent of the cathode surface area and electrode separation distance. This shows that implant design considerations need not be constrained by these cathode design parameters.

Evaluation of a Multi-metal Approach to Iontophoretic Antibacterial Prophylaxis and Treatment in Orthopaedic Implants

by
Anirudh Ramnath Ganapathy

A thesis submitted to the Graduate Faculty of
North Carolina State University
in partial fulfillment of the
requirements for the degree of
Master of Science

Industrial Engineering

Raleigh, North Carolina

2013

APPROVED BY:

_____	_____
Dr. Rohan A. Shirwaiker Committee Chair	Dr. Richard A. Wysk
_____	
Dr. Paul E. Orndorff	

BIOGRAPHY

Anirudh Ramnath Ganapathy was born on 2nd September, 1989, in Chennai, India. He received his Bachelor's Degree in Mechanical Engineering from Vellore Institute of Technology, India, in 2011. He is currently pursuing his Master's Degree in Industrial Engineering at North Carolina State University, Raleigh, NC. His current research is in antibacterial orthopaedic implant design under the guidance of Dr. Rohan A. Shirwaiker.

ACKNOWLEDGMENTS

At the outset, I thank my advisor Dr. Rohan A. Shirwaiker, who provided me with the opportunity to be part of something novel and exciting. As a mentor and guide, he has been a prime motivational force, and if I have managed to accomplish my research goals, it is due to his guidance and counsel.

I would like to express my gratitude to the members of my advisory committee, Dr. Richard A. Wysk and Dr. Paul E. Orndorff, for their support and encouragement, and their generosity in granting me the full and unrestricted use of their laboratory facilities.

I am grateful to researchers Mrs. Patty Spears and Ms. Mitsu Suyemoto, whose guidance in the laboratory was instrumental in the completion of the experimentation phase of my research.

I owe a large debt of gratitude to my fellow graduate students: Zhuo Tan, without whose patient instruction I would never have learnt to develop my experimental protocols; and Priyanka Sheshadri and Nikil Kumar, whose statistical expertise proved invaluable.

I'm grateful to all my friends whose company and sense of humor kept me sane during the most stressful of times.

I am most grateful to my parents and family, whose constant support, encouragement, and love has kept me going all these years, and will continue to do so for all my life.

TABLE OF CONTENTS

LIST OF TABLES ..... **vi**

LIST OF FIGURES ..... **vii**

CHAPTER 1: INTRODUCTION **1**

1.1 Background **1**

1.2 Motivation **6**

1.3 Research Objectives **9**

1.4 Thesis Outline **11**

1.5 Chapter Summary **11**

CHAPTER 2: LITERATURE REVIEW **13**

2.1 History of Silver as an Antibacterial **13**

2.2 Mechanisms of Antibacterial Action **14**

2.3 Cytotoxicity of Silver **17**

2.4 Silver-based Medical Devices: The State of the Art **20**

2.5 Iontophoretic Silver-based Antibacterial Implants **23**

2.6 Chapter Summary **25**

CHAPTER 3: METHODOLOGY AND EXPERIMENTATION **27**

3.1 System Design **27**

3.2 Testing Methodology **30**

3.2.1 Testing Setup **30**

3.2.2 Bacterial Preparation and Inoculation Protocol **36**

3.3 Statistical Empirical Design: Testing with *S. aureus* **37**

3.4 Validation Study: Testing with *E.coli* **38**

3.5 Chapter Summary 39

CHAPTER 4: RESULTS AND ANALYSIS 41

4.1 Experimental Results 41

4.2 Statistical Analysis 44

4.2.1 Statistical Analysis of Results for *S. aureus* 44

4.2.2 Statistical Analysis of Results for *E. coli* 48

4.3 Discussion 49

4.4 Chapter Summary 54

CHAPTER 5: CONCLUSIONS AND FUTURE WORK 56

5.1 Conclusions 56

5.2 Future Work 57

REFERENCES 62

APPENDICES 74

APPENDIX A: Observations from Experiments on *S. aureus* 75

APPENDIX B: Observations from Experiments on *E. coli* 78

APPENDIX C: Additional Experimental Results 79

APPENDIX D: Images of Experiments on *S. aureus* 80

APPENDIX E: Images of Experiments on *E. coli* 88

LIST OF TABLES

Table 1.1 FDA Classification for Medical Devices 3

Table 1.2 Classification of Prosthetic Joint Infections 7

Table 1.3 Commonly Identified Microorganisms in Orthopaedic Infections 7

Table 2.1 Effects of Silver Toxicity in Mammalian Cells 19

Table 2.2 Commercially available Silver-based wound dressings 21

Table 3.1 List of Materials, Functions, Specifications and Suppliers 34

Table 3.2 System Constant Parameters and Values 35

Table 3.3 System Configurations and Levels for experimental setup 35

Table 3.4 Summary of the system configurations in a single replication of the Empirical Design for testing with *S. aureus* 38

Table 3.5 Summary of the system configurations in a single replication of the Validation Study for testing with *E. coli* 39

Table 4.1 Inhibition Zone Areas (in mm^2) for *S. aureus* 43

Table 4.2 Inhibition Zone Areas (in mm^2) for *E. coli* 44

Table 4.3 Three-Factor Statistical Design Parameters 45

Table 4.4 Single-Factor Statistical Design Parameters 49

Table 4.5 Prices of Silver, Titanium and Stainless Steel 52

Table 4.6 Average Inhibition Zone Areas in *S. aureus* over three replications 52

Table 4.7 Average Inhibition Zone Areas in *E. coli* over three replications 53

LIST OF FIGURES

Figure 1.1 Projected rise in number of Total Hip Arthroplasties and Total Knee Arthroplasties between 2005 and 2030 2

Figure 1.2 (a) and (b) Two views of an external fixator with a temporary two-ring frame 4

Figure 1.3 Internal fixator to fix fractures in both bones of the forearm 5

Figure 2.1 (a) *E. coli* prior to Ag^+ treatment 16

Figure 2.1 (b) Cell wall separation and condensed DNA molecules 16

Figure 2.1 (c) Presence of Ag^+ within cell and cell wall 16

Figure 2.2 (a) A patient with argyria presenting with bluish-gray skin 18

Figure 2.2 (b) A biopsy of his skin revealing silver deposits in the dermis 18

Figure 2.3 (a) MUTARS®Silver silver-coated proximal femur replacement with a bipolar cup 22

Figure 2.3 (b) post-operative x-ray of the megaendoprosthesis 22

Figure 3.1 Schematic Representation of Experimental Setup 29

Figure 3.2 Electrode Assemblies 31

Figure 3.3 Electrodes held in position using scotch tape 32

Figure 3.4 Prepared agar plate with electrodes inserted and held in place with wax 33

Figure 3.5 Complete Experimental Setup 37

Figure 4.1 Inhibition Zone Shape-Based Area Calculation 41

Figure 4.2 Measurement of Inhibition Zone Area 42

Figure 4.3 ANOVA Table from RStudio Output for *S. aureus* 46

Figure 4.4 Residuals vs. Fitted Values Plot for *S. aureus* 46

Figure 4.5 Normal Probability Plot of Residuals for *S. aureus*.....47

Figure 4.6 RStudio Summary of Fitted Model for *S. aureus*.....48

Figure 4.7 ANOVA Table from RStudio Output for *E. coli* 49

Figure 4.8 Average Inhibition Zone Areas for experiments on *S. aureus*.....53

Figure 4.9 Average Inhibition Zone Areas for experiments on *E. coli*.....54

Figure 5.1 Inhibition Zones in experiments with 25 mm Anode and Cathode Lengths 60

CHAPTER 1: INTRODUCTION

1.1 Background

The Medical Device Directives (MDD) defines a medical device as follows:

"*Any instrument, appliance, apparatus, material or other article, whether used alone or in combination, including the software necessary for its proper application, intended by the manufacturer to be used for human beings for the purpose of*

- *Diagnosis, prevention, monitoring, treatment or alleviation of disease*
- *Diagnosis, monitoring, alleviation of or compensation from an injury or handicap*
- *Investigation, replacement or modification of the anatomy or of a physiological process*
- *Control of conception*

and which does not achieve its principal intended action in or on the human body by pharmacological or immunological or metabolic means, but which may be assisted in its function by such means" [1].

Medical device manufacturers develop and manufacture a vast variety of products, ranging from simple rubber examination gloves to complex cardiac pacemakers and imaging machines. The global medical device industry provides life-enhancing treatments and technology and drives the US and global economy with its emphases on manufacturing and R&D. The medical device industry in the US provides employment to 2.4 million people directly and indirectly, and the global market is worth $350 billion [2].

Medical and scientific advances in the last few decades have increased overall life-expectancy. As the baby-boomer generation is reaching their late middle- to senior ages, the demand for life-sustaining medical technology has seen a steep increase. This

demographic is only expected to grow in size, with the Census Bureau predicting the number of people older than 65 to be 54 million by 2020, and 86 million by 2050 [3].

The increase in the number of medical device related surgeries over the years is an indication of the extent to which medical devices have improved quality of life. For example, there has been an increase in the use of implantable cardiac rhythm management devices such as Pacemakers over the past two decades; the number of Pacemaker implantations in the US rose from 121,300 in 1993 to 188,700 in 2009, a 56% increase [4]. Similarly, statistics collected by the Center for Disease Control and Prevention (CDC) show a steep increase in the number of joint prosthesis surgeries in the past 5 years. ~676,000 total knee arthroplasties (TKA) and ~327,000 total hip arthroplasties (THA) were performed in 2009, as compared to an estimated 600,000 joint prosthesis surgeries performed in 2004 [5]. Furthermore, projections show that between 2005 and 2030, the number of THA and TKA is expected to grow by 174% and 673%, respectively [6]. These numbers strongly reflect the growing dependence of healthcare on medical devices designed to improve the quality of life of patients with life-altering injuries or medical conditions.

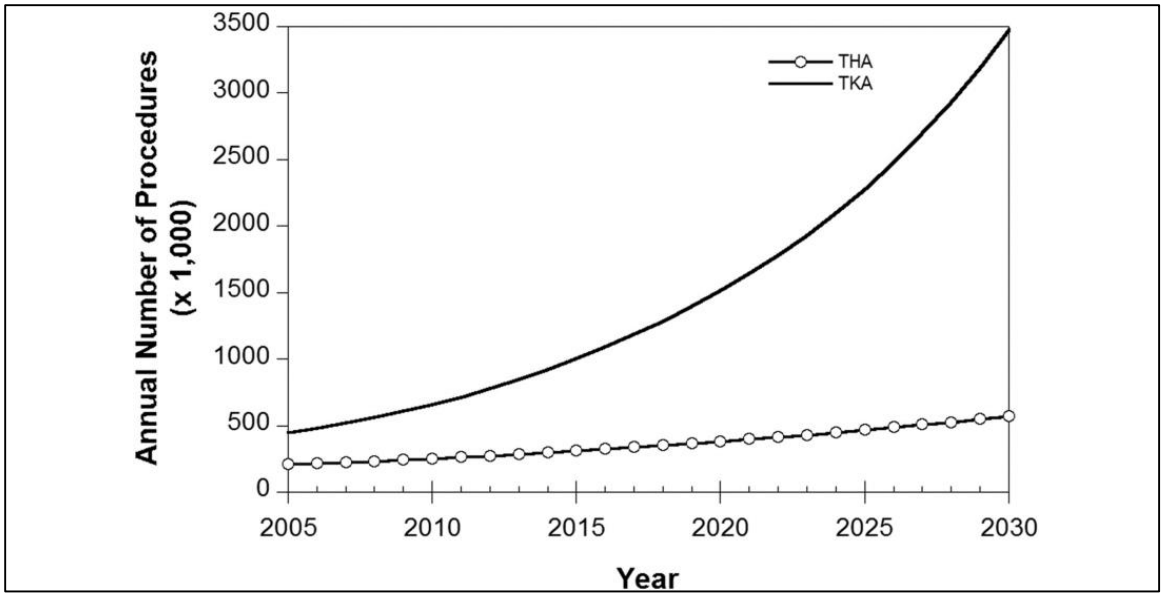

Figure 1.1 Projected rise in number of Total Hip Arthroplasties and Total Knee Arthroplasties between 2005 and 2030 [6]

In order to assure the safety and effective functioning of medical devices, the U.S. Food and Drug Administration (FDA) classifies them into 3 categories based on the level of control deemed necessary. The Code of Federal Regulations Title 21 (21 CFR), governs the classification procedures [7]. Table 1.1 summarizes the FDA classification of medical devices, the level of control specified, and the rationale behind classification [8].

Table 1.1 FDA Classification for Medical Devices [8]

Class	Controls	Reasoning
Class I	General Controls only	Minimum potential harm to user
Class II	General Controls with Special Controls	More than minimal potential harm, special controls are needed to ensure safety
Class III	General Controls with Special Controls and Premarket Approval (PMA)	Insufficient information exists to ensure safety and effectiveness, pre-market approval is needed

Orthopaedic implants are medical devices which are used to replace or support a missing or damaged bone or bone joint. A wide variety of orthopaedic implants exist which replace or support various bones or joints in the body. The most common forms are pins, rods, screws and plates which anchor fractured bones while they heal, but other complex implants exist which replace entire joints like the knee and the hip. Although orthopaedic implants are classified as Class I, II, or III medical devices under FDA guidelines based on the identified risks of infection, adverse tissue reaction, pain and/or loss of function etc. [9], most orthopaedic implants on market fall under Class III [8].

Based on the application, orthopaedic implants may be classified as external fixators and internal fixators. External fixators use pins or wires laced through holes drilled into bone

and secured to external scaffolding. This kind of fixation is used in indications where it is necessary to stabilize open fractures, correct misalignments, heal closed fractures with severe soft tissue injuries etc. The main advantages offered by external fixators are:

- minimal disruption of soft tissues and blood supply
- the ability to avoid implant fixation into infected areas
- post-operative adjustability [10]

The external fixator shown in Figures 1.2 (a) and (b) consists of a temporary two-ring frame that provides provisional stability as well as allows access to soft tissue for treatment. It also allows for follow-up treatment to the bones [10].

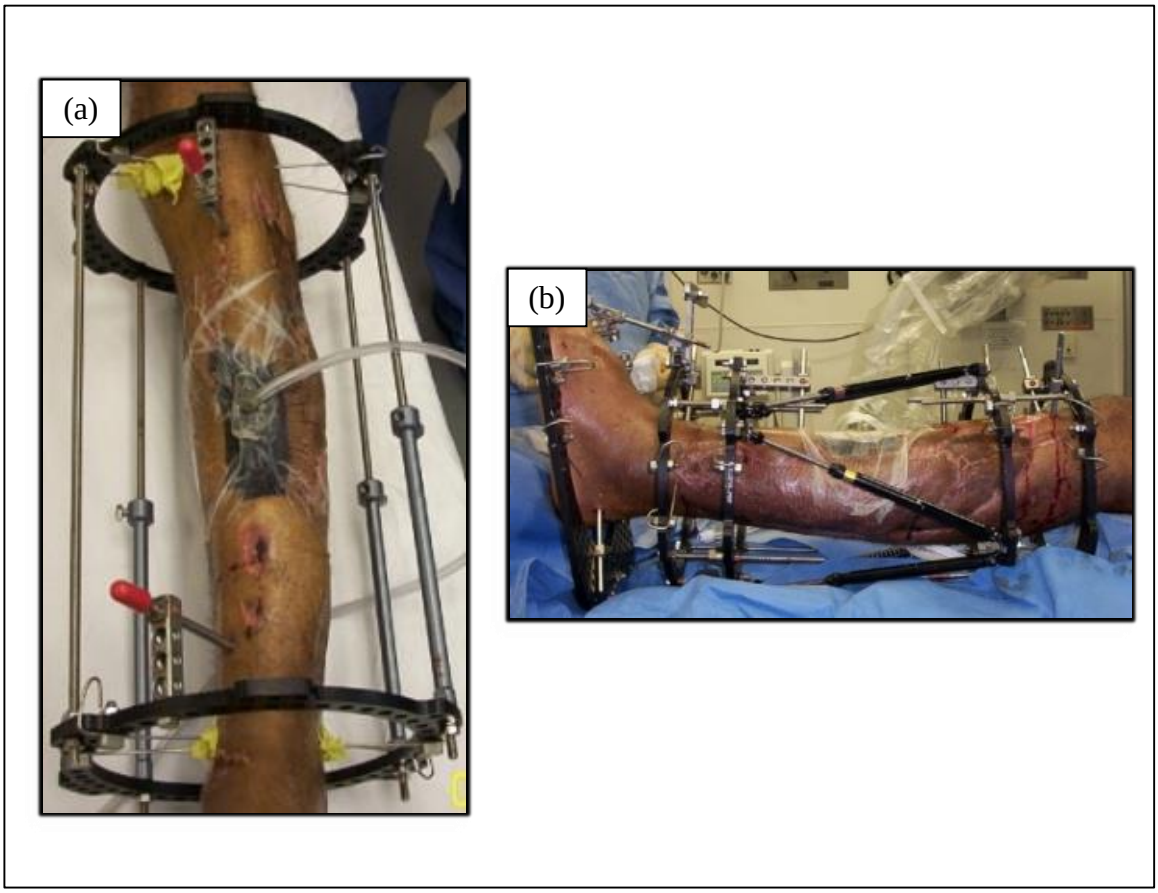

Figure 1.2 (a) and (b) Two views of an external fixator with a temporary two-ring frame [10]

Internal fixators are applied to bones by surgically applying implants. Open surgery is performed to manipulate the bones or implant components into the right position. Screws, plates, pins or intermedullary rods are then used to hold the bones or implant components in place. Internal fixation is indicated in cases when severe damage (often caused by trauma) affects bloody supply to the fracture and there is potential for bone or soft tissue necrosis to occur. Internal fixation offers the following advantages:

- flexibility and precision in the fixation process
- faster healing of fractures
- reduced likelihood of refracture [11]

Figure 1.3 shows internal fixators used to fix fractures of both bones of the forearm. Panel A shows a pre-operative X-ray of the forearm showing a fracture in both bones. Panel B shows an X-ray following surgical fixation using a Locking Compression Plate. Panel C shows two views of the bones after 10 months of follow-up showing fracture union [12].

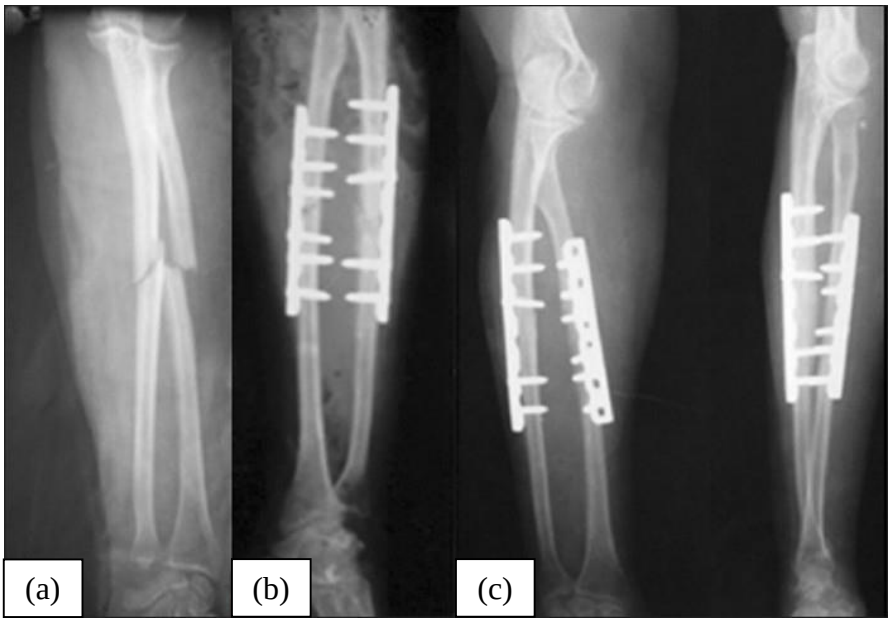

Figure 1.3 Internal fixator to fix fractures in bones of the forearm [12]

1.2 Motivation

A major complication associated with orthopaedic implants is the risk of infection. Infection is one of the leading causes of arthroplasty failure, with an incidence of 1.5-2.5% for primary interventions and up to 20% for revision procedures [13]. Across the board, an average of 5% of all primary internal fixation devices become infected. With external fixators, risk of infection is highest at the pin site, occurring in 11% of patients [14].

While the percentage of incidence of prosthetic joint infections appears to be low, the sheer number of orthopaedic surgeries performed every year implies dire ramifications in terms of the associated medical costs and discomfort to patients. The accurate diagnosis of infection in orthopaedic devices usually requires a combination of clinical, laboratory, histopathology, microbiology, and MRI and CT imaging studies. Treatment may require surgical procedures including implant removal, debridement of infected tissue, implant replacement, and 6-12 weeks of antimicrobial therapy [14]. Revision TKA caused by infection have an average cost of $109,805, as opposed to the $55,911 for revision TKA performed for other causes [15]. In addition, the mortality rate due to orthopaedic infections is between 1% and 3% [13].

The majority of infections affecting fracture-fixation devices and surgically inserted orthopaedic implants are hospital acquired (HAIs). An estimated 60% of prosthetic joint infections are acquired by direct contamination during surgical procedures. The risk of infection is increased by necrosis and open trauma. The type of infection and subsequent treatment required is dependent on the time of onset after surgery. Table 1.2 classifies infections based on time of onset, and summarizes stage of acquisition and treatment options [16].

The most common organisms responsible for prosthetic joint infections are Gram-positive staphylococcal bacteria, constituting more than 50% of all isolates. *Staphylococcus aureus* is alone responsible for 30% of infected prosthetic implants, while

coagulase-negative staphylococci are responsible for another 22% of infections. Table 1.3 summarizes commonly identified microorganisms responsible for infections in orthopaedic devices [14].

Table 1.2 Classification of Prosthetic Joint Infections [16]

Category	Early	Delayed	Late
Presenting after surgery	1 month	2-6 months	> 6 months
Acquisition	During implantation	During implantation	Haematogenous
Aetiology	*Staphylococcus aureus, Streptococcus* spp., GNB	*Staphylococcus epidermis*	*Staphylococcus aureus, Streptococcus* spp., *Staphylococcus epidermis,* bacilli
Treatment	Retention	Removal	Retention

Table 1.3 Commonly Identified Microorganisms in Orthopaedic Infections [14]

Microorganism	**Frequency (%)**
Staphylococcus aureus	30
Coagulase-negative *staphylococci*	22
Gram-negative *bacilli*	10
Anaerobes	5
Enterococci	3
Streptococci	1
Polymicrobial	27
Unknown	2

The management of infections in prosthetic joints must be done on a case-by-case basis, as the optimal treatment depends on multiple factors: stability of prosthesis, infection type and causative organism, surgical limitations, possibility of oral treatment etc. [16]. In terms of prophylaxis, sterile surgical techniques and intravenous administration of antibiotics such as cefazolin, cefuroxime and vancomycin are the current standard of care in orthopaedic surgery [17]. However, these solely do not prevent the risk of postoperative infections. In fact, the prolonged and rampant use of antibiotics to fight infections has led to the evolution of resistant strains of bacteria like Methicillin-resistant *S. aureus* (MRSA). These "superbugs" are far more difficult to treat than their corresponding non-resistant strains. Furthermore, there are concerns that the regular prescription of antibiotics to fight infections will precipitate the evolution of more such resistant strains of commonly occurring pathogens.

The lack of well-defined prosthetic joint infection treatment protocols, combined with the dangers of antibiotic-resistant strains of pathogens, indicates the necessity for a non-antibiotic system to deal with implant infections. An alternative to antibiotics is treatment with the oligodynamic metal, silver, which has long been considered to have antimicrobial characteristics. There exists anecdotal and experiential evidence to suggest its effectiveness against infections [18]. Silver sulfadiazine has been used in wound dressings and to treat external infections [19], and has also been used to coat catheters and endotracheal tubes [20] [21]. There has been, however, no hard evidence to support the antimicrobial efficacy of silver in its native form. Elemental and colloidal silver have shown limited antibacterial activity in aqueous environments. It has been found that the antibacterial efficacy of suspended silver is inversely related to the size of the suspended particles at very low concentrations [22].

High antibacterial efficacy has been shown by electrically generated silver ions using direct current. This method of release is advantageous as it can be used for continuous localized release of silver ions without being dependent on environmental conditions. Spadaro et al. tested the effects of relatively weak direct currents in silver electrodes on

four different kinds of bacteria, and found significant levels of inhibition of bacterial growth in all four strains. Similar tests were also performed with other electrode materials (e.g., platinum, gold and stainless steel), and much higher currents were noted to be required to achieve similar effects [23]. Fuller et al. characterized the operational parameters of an iontophoretic antimicrobial system using electrically activated silver electrodes to inhibit bacterial growth, and effectively tested the system *in vivo* using an osteomyelitic rat model [24] [25].

However, there exist concerns about the potential harmful effects of overexposure to silver. The most common adverse effects of overexposure to silver are argyria and argyrosis. Other known adverse effects include liver and kidney damage, irritation of the eyes, skin, respiratory and intestinal tract, and changes in blood cells [26]. It has been documented that ionic silver retains cytotoxicity against mammalian cells at concentrations of 1 mg/L [27]. The Permitted Exposure Limit (PEL) recommended by the Occupational Safety and Health Administration (OSHA) and the National Institute for Occupational Safety and Health (NIOSH) is 0.01 mg/m^3 for all forms of silver [26]. Hence, there is a necessity to control and minimize the amount of silver used in an iontophoretic technology to be suitable for orthopaedic implantable devices. Accordingly, this thesis focuses on evaluating the feasibility and effectiveness of a system design configuration that minimizes the quantity of silver in the system without potentially compromising its antibacterial efficacy.

1.3 Research Objectives

Prior research by Fuller et al evaluated a system to exploit the antibacterial properties of low intensity direct current (LIDC) activated silver to prevent bacterial infections in orthopaedic implants [23]. Their system was configured entirely out of silver; silver wires served as both anode and cathode (Ag-Ag electrode configuration). Their results demonstrated that the material of the anode contributed more significantly to the antibacterial efficacy of the system than the material of the cathode, as bacterial

inhibition zones only formed around the anodes. This suggests that the bactericidal effects of the system may not be affected by using a cathode of a different material. A non-silver cathode material would be advantageous for two reasons:

1. The toxicity of silver – using less toxic and more biocompatible materials will reduce the risk of the adverse health effects of overexposure to silver

2. The high cost of silver – it would be economically advantageous to substitute a cheaper material provided the antibacterial properties remain unaffected

The materials chosen for the cathodes in this research are titanium (Ti) and stainless steel (SS). Both these materials have been prominently used in biomedical (especially orthopaedic) applications for many years because of their desirable characteristics including biocompatibility, the ability to osseointegrate, and a suitable Young's modulus which closely matches that of human bones [28].

The specific objectives of the research enumerated in this thesis are as follows:

- Develop and evaluate an alternative system configuration of an iontophoretic LIDC activated antibacterial system for orthopaedic implants by using different electrode material combinations (anode-cathode configurations: Ag-Ti and Ag-SS), and compare their effectiveness with the prior Ag-Ag electrode configuration.

- Assess the effects of two design parameters, electrode separation and cathode surface area, on the antibacterial efficacy of the proposed alternative configurations. Fuller et al found these parameters to not contribute significantly in the case of the original Ag-Ag configuration, but no data exists to determine their effect in electrode configurations using dissimilar metals.

The antibacterial efficacy of the proposed multi-material configurations will be tested against *S. aureus* (Gram-positive) using a statistical empirical design. In order to verify

that the multi-metal iontophoretic antibacterial device displays the same behavior against Gram-negative bacterial species, a validation study is performed by testing its performance against *Escherichia coli*.

1.4 Thesis Outline

Chapter 2 reviews the existing literature on the uses of silver in medical applications, the antibacterial mechanisms of silver, the cytotoxic effects of silver, currently available silver-based medical devices, and the development of iontophoretic silver-based antibacterial implants. Chapter 3 describes the system design and materials used for experimentation, testing setup and protocols, and statistical empirical design. Chapter 4 discusses the results of the experimentation, statistical analysis, and interpretation of the results. Chapter 5 presents the conclusions and directions for future research based on these results.

1.5 Chapter Summary

The healthcare industry has become increasingly dependent on medical devices to improve the effectiveness of medical care and quality of life of patients. With increasing life expectancy and a growing population of senior citizens, the use of implantable medical devices and prosthetics has already started to rise steeply. Infections acquired during the process of implantation or post-implantation cause very serious complications, and are difficult to diagnose and treat. The diagnosis and treatment of orthopaedic infections is extremely expensive, and causes additional pain and suffering to patients. While treatment of infections with antibiotics continues to be the primary standard of care, there are growing concerns about the evolution of antibiotic-resistant *superbugs* like MRSA which are extremely difficult to treat due to antibiotic overuse. There is an immediate need for non-antibiotic-based antibacterial devices for prophylaxis and treatment to prevent the occurrence of post-operative orthopaedic infections. Research has shown that ionic silver released locally by the application of LIDC can inhibit bacterial growth and hence prevent infection. However, silver is toxic to living cells

beyond a threshold concentration, and hence its quantity in an implantable device must be minimized without compromising antibacterial efficacy. This thesis explores the feasibility of reducing the amount of silver in the iontophoretic antibacterial device by partially substituting silver with standard biocompatible metals. The antibacterial efficacy of the new device design configuration is evaluated and compared to the original design using a statistical empirical design.

CHAPTER 2: LITERATURE REVIEW

2.1 History of Silver as an Antibacterial

Silver has been used in many forms for medical applications over centuries. Silver containers were thought to preserve food and water and keep them fresh for longer. The ancient Macedonians used silver plates to achieve improved wound healing and prevent post-operative infection [29]. In the 18th century, silver nitrate was used in a hardened form, i.e. "lunar caustic", to remove granulation tissue from slowly healing or unhealed wounds. Early in the 19th century, silver nitrate in different forms, including as a 0.2-2% solution, was used to treat fresh burns. Towards the end of the 19th century, the medical applications utilizing antibacterial properties of metallic silver became more prominent. Silver foil was used as a dressing on wounds. Silver nitrate solution was used to treat eye infections in newborns. Both these forms were also used in the treatment of infected burns [30]. In the first half of the 20th century, a combination of tannic acid and silver nitrate was proposed and widely used in the treatment of burns, notably as a treatment for battlefield wounds during the World Wars [31].

The discovery and development of penicillin-based antibiotics precipitated a lack of interest in silver-based antimicrobial treatments until the 1960s. The use of 0.5% silver nitrate as a treatment for burns was introduced by Moyer [32]. It was found to have antibacterial properties against *S. aureus, Pseudomonas aeruginosa* and *E. coli*. In 1968, silver sulfadiazine was introduced as a broad-spectrum antibacterial treatment against burns [33]. Silver sulfadiazine is still widely used in the treatment of burns as topically applied creams, wound dressings etc. under various brand names like Silvadene®, SSD Cream®, and Thermazene® [34]. However, recent findings have indicated that silver sulfadiazine delays wound-healing [19].

It is known that the antimicrobial action of silver is related to the release of its ion (Ag^+), and not its elemental form [35]. Colloidal and aqueous solutions of silver have shown limited antibacterial efficacy due to the displacement of Ag^+ ions from the solution. The

antibacterial efficacy of suspended silver was found to be inversely related to the size of the suspended particles at low concentrations [22]. In recent years, research in the use of silver nanoparticles (Ag-NPs) for medical purposes has achieved some significant results. Ag-NPs have been found to have excellent antibacterial action [36] [37]. Commercial products like Acticoat® [38] , an antimicrobial barrier dressing, are available which inhibit bacterial growth through the release of Ag^+ ions from Ag-NPs [39].

2.2 Mechanisms of Antibacterial Action

Several theories have been proposed to explain silver's antibacterial mechanisms. It must be noted that silver, in its metallic form, is inert. The antibacterial action of silver is primarily attributed to its ionized form. In the case of applications such as wound dressings, presence of moisture in the skin and fluids from wounds, silver gets ionized [40].

Schreurs and Rosenberg studied the effect of Ag^+ ions on the transport of essential nutrients within bacterial cells in *E. coli*. They proposed that the binding of Ag^+ ions causes the collapse of the combined cellular energy resources to an extent that maintaining the concentration of critical metabolites is no longer possible, interfering with the respiratory chain. Furthermore, pertinent to transport phenomena, the Ag^+ ions interfere with specific carriers such as thiol groups (-SH) [41]. Ghandour et al proposed that Ag^+ ions bind to essential sites such as proteins and enzymes within the bacterial cells by displacing native metal cations, thus rendering them inactive. These mechanisms affect cell metabolism and lead to cell death [42].

Another bactericidal mechanism proposed in previous literature is the effect of Ag^+ ions on the cell wall and membranes. Lansdown suggested that the positively charged Ag^+ ions attach themselves to the slightly negatively charged bacterial cell wall causing structural destabilization in the cell wall and intracellular membranes. Ag^+ adhesion to the cell wall leads to changes in the osmotic pressure within the cell, causing the cell wall to break down and leak the cell's contents [43]. Dibrov et al experimentally demonstrated

the ability of Ag^+ ions to collapse the proton motive force on the cell membrane, interrupting ionic transportation which is dependent on the membrane [44].

Feng et al studied the effect of silver nitrate treatment on *E. coli* and *S. aureus* using Transmission Electron Microscopy (TEM) and X-ray microanalysis. They found that under the action of Ag^+ ions liberated from silver nitrate, the cytoplasm membrane had detached from the cell wall. An electron-light region appeared in the center of the cells which contained condensed DNA molecules. X-ray microanalysis indicated the presence of silver in electron-dense granules surrounding the cell walls and deposited inside the cells. The condensed state of the DNA molecules indicated a loss in replication ability, and this was confirmed by a lack of cell multiplication during continuous cultivation. Furthermore, the presence of silver in the cells indicated the inactivation of bacterial proteins by Ag^+ ion interactions with thiol groups [45].

Figure 2.1(a) shows the structure of an *E. coli* cell prior to treatment with Ag^+ ions. The arrow indicates the electron-light DNA molecules. Figure 2.1(b) shows the electron-light condensed DNA molecules after treatment with Ag^+, and the separation between the cell wall and the cytoplasm membrane. Figure 2.1(c) shows the presence of electron-dense granules of silver near the cell wall and within the cell [45].

The literature presented suggests that the antibacterial effect of silver is not caused by any one single mechanism, but a multipronged manner of attack. In summary, Ag^+ ions act on bacteria and cause cell death in the following ways:

a) Inactivation of proteins and enzymes which inhibits cell metabolism and respiration

b) Disruption of the cell wall and cytoplasmic membrane by adhesion of Ag^+ ions to the cell wall, and interruption of membrane-based ion transportation

c) Destruction of the replication abilities of DNA, inhibiting cell replication.

The action of any antibiotic against bacteria is generally restricted to a single mechanism, as compared to the multiple modes of action of Ag^+ ions. While it is relatively easier for bacteria to develop mutations to resist a single mechanism, and hence antibiotic resistance, the possibility of bacterial species developing resistance to multi-modal Ag^+ ions is restricted.

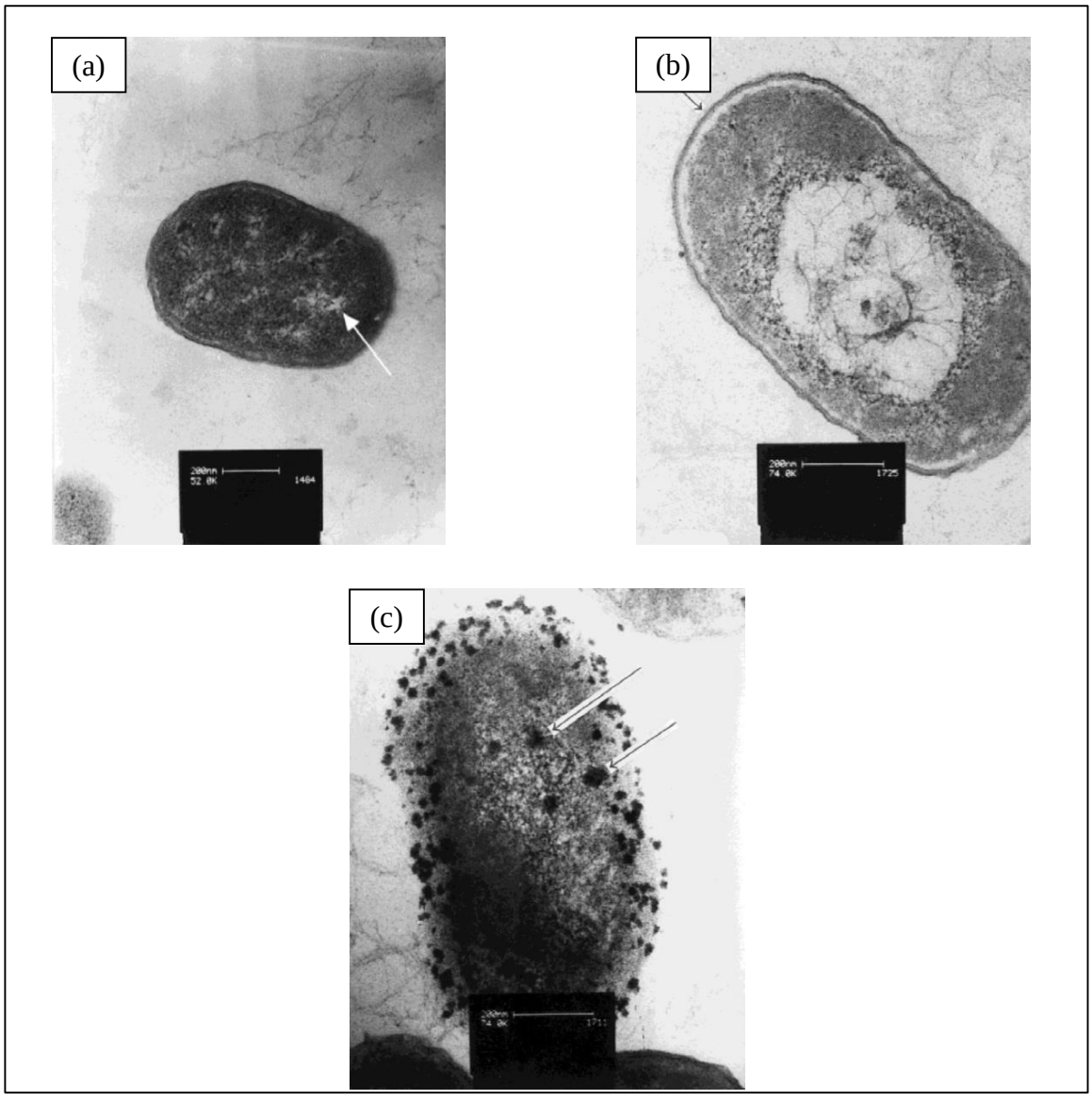

Figure 2.1 (a) *E. coli* prior to Ag^+ treatment, (b) Cell wall separation and condensed DNA molecules, and (c) Presence of Ag^+ within cell and cell wall [42]

2.3 Cytotoxicity of Silver

While there are no disputes about the antibacterial effectiveness of silver, a major concern with its usage in medical devices is the potential adverse health effects. The best known and most common effect of over-exposure to silver is argyria, caused due to the accumulation of silver over time in the soft tissues of the skin, liver and spleen [46]. Though documented cases of argyria have existed since the 1st Century A.D., the term "Argyria" itself was first used in 1840 [47]. Overuse of silver-based treatments like "argyrol" and "neo-silvol" leading to undiagnosed cases of argyria have been mentioned in literature as early as 1941 [48]. Argyria is indicated by a bluish-gray hue of the skin, and as such, is considered a benign condition by the Agency for Toxic Substances and Disease Registry (ATSDR) of the CDC as only a "cosmetic" problem [49].

Silver is absorbed in the human body in different forms, and the form in which it is absorbed may affect the intensity of argyrial effects. However, the mechanism of formation of argyrial deposits is dependent on the release of Ag^+ ions. Liu et al studied the mechanism of formation of argyrial deposits in the human body [50]. It was found that Ag^+ ion release occurs in the GI tract due to the low pH, and the Ag^+ ions complex with thiol groups and proteins. These ions and complexes enter the bloodstream and circulate systematically. When exposed to light in the near-skin regions, Ag^+ ions are easily photoreduced to metallic silver and deposited, causing the bluish-gray appearance associated with argyria. Figure 2.2 shows the effects of argyria (bluish-gray skin) as seen in a patient [47].

Exposure to silver has also been found to have potentially more serious health-adverse consequences than the merely cosmetic effects of argyria [26] [51] [52]. Consumption of large quantities of colloidal silver has been linked to pleural edema, hemolysis, and toxicity to bone marrow. Toxic effects similar to those experienced on consumption of corrosive solutions have also been observed on oral exposure to high doses of inorganic silver. These include burning of the throat, abdominal pain, vomiting, diarrhea, and the

onset of convulsions and shock. Intravenous administration of inorganic silver has been found to impact the functioning of the central nervous system, manifested as weakness in limbs and loss of motor function, as well as cardiac conduction [47]. In order to control exposure to silver, the Environmental Protection Agency (EPA) has published an oral reference dose (RfD) of 5 µg/kg/day. This dose is an estimate of the maximum amount of silver a human can be exposed to on a daily basis without experiencing any appreciable adverse medical effects over a lifetime [53]. Table 2.1 summarizes some of the evidence of silver toxicity in mammalian cells [54].

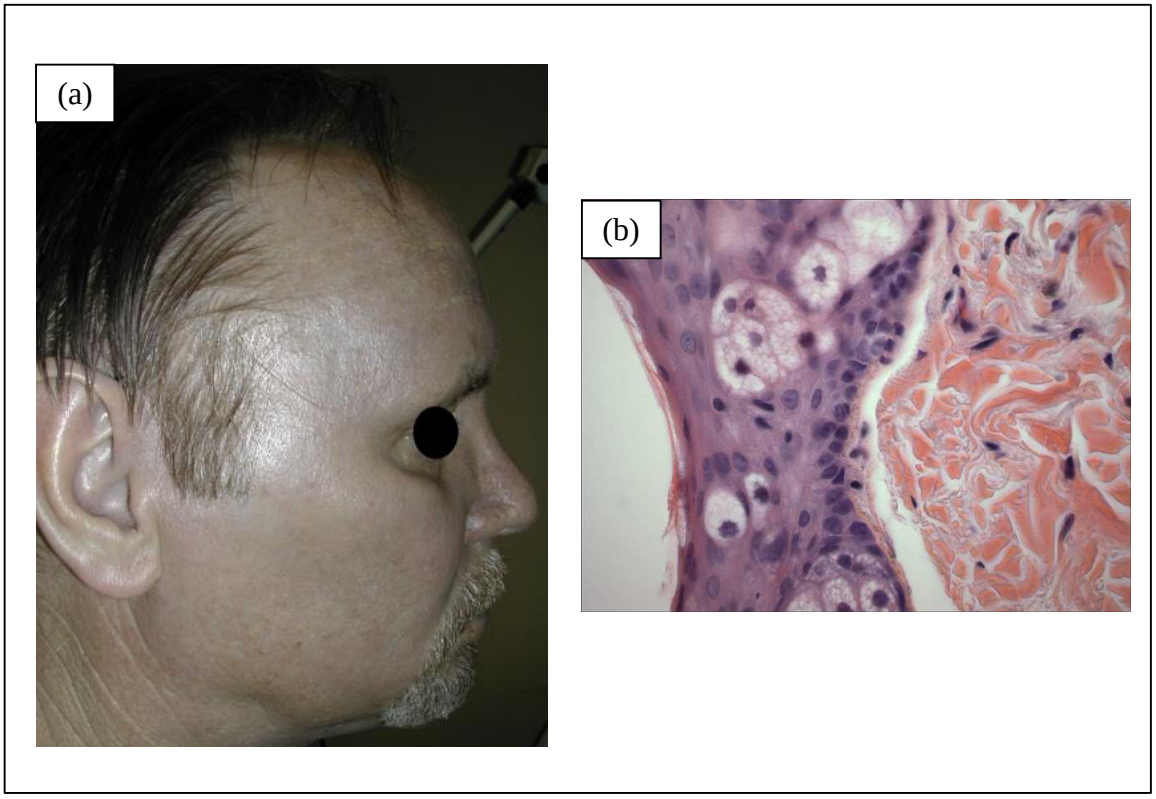

Figure 2.2 (a) A patient with argyria presenting with bluish-gray skin, and (b) A biopsy of his skin revealing silver deposits in the dermis [47]

Table 2.1 Effects of Silver Toxicity in Mammalian Cells [54]

Target cell/Organism	Key aspects
Rat lung cells	Reduction in lung function and inflammatory lesions
Sprague-Dawley rats	Ag-NPs accumulation in olfactory bulb and subsequent translocation to the brain
Mouse stem cells	Cell leakage and reduction of mitochondrial function
Rat liver cells	Cell leakage and reduction of mitochondrial function
Human fibrosarcoma and human skin/carcinoma	Oxidative stress. Low doses produced apoptosis and higher dose necrosis
Mouse fibroblast	50 μg/mL induced apoptosis to 43.4% of cells
Human colon cancer	100 μg/mL produced necrosis in 40.2% of cells
Human glioblastoma	Ag-NPs were found cytotoxic, genotoxic and antiproliferative
Human fibroblast	Ag-NPs were found cytotoxic, genotoxic and antiproliferative

Drake and Hazelwood proposed that metallic silver posed a minimal health risk [26]. However, Danscher and Locht countered this suggestion, proposing instead that the implantation of silver or silver-plated devices is not recommended, as the number of Ag^+ ions released is proportional to the size and surface area of the implanted silver [55]. Thus, there is ample motivation to minimize the quantity of silver in implantable systems such as the one that uses low intensity direct current (LIDC) to release Ag^+ ions from metallic silver [24]. To achieve this purpose, this thesis explores the substitution of the silver cathode with other biocompatible and non-toxic materials, which will not potentially compromise the antibacterial efficacy of the system. The cathode materials

selected for the proposed alternate design are titanium and stainless steel. These two materials fulfill the biomechanical requirements of prosthetics, and are the most commonly used materials in commercial orthopaedic implants and implantation systems [56] [57] [58] [59] [60] [61]. Titanium is biocompatible, non-toxic, possesses the ability to osseointegrate, and has a Young's Modulus very similar to that of bone [28]. These properties make it an ideal material to be used in long-term orthopaedic implants. Stainless steel shares similar biomechanical properties, but can be mildly cytotoxic due to the presence of Nickel. However, the level of cytotoxicity is very low even at high concentrations, and is deemed safe for implantation [62]. Hence, stainless steel is suitable for use in temporary implants [63].

2.4 Silver-based Medical Devices: The State of the Art

The use of silver in different forms as an antibacterial has become widespread in the past few decades, with several commercially available FDA-approved medical products claiming superior antimicrobial capabilities due to the presence of silver. The most common products are antibacterial silver-containing wound dressings, but other devices like silver-coated catheters, endotracheal tubes and certain prosthetics have also been introduced.

Hiro et al performed a comparative evaluation of 9 different silver-based antimicrobial dressings [64]. They observed that while all the silver-containing dressings accelerated the wound-healing process by effectively killing the tissue bacterial load, the individual responses to bacterial killing and wound healing varied widely. Cytotoxicity to fibroblasts and keratinocytes was also reported. Several other studies have also evaluated the effectiveness and biocompatibility of silver-based wound dressings [65] [66] [67]. These results indicate a lack of a quantifiable and controllable release of Ag^{+} ions.

Table 2.2 lists a few commercially available wound-dressings that contain silver to fight bacterial action [39].

Table 2.2 Commercially available Silver-based wound dressings [39]

Name	Manufacturer	Nature of Product
Acticoat	Smith and Nephew, London, UK	Nanosilver-coated polyethylene
Actisorb	Johnson and Johnson, New Brunswick, USA	Silver nylon cloth/activated charcoal
Aquacel Ag	ConvaTec, Skillman, USA	Silver-impregnated carboxymethylcellulose
Askina Calgitrol Ag	B. Braun, Melsungen, Germany	Silver alginate
Contreet	Coloplast, Minneapolis, USA	Silver hydrocolloid
PolyMem Silver	Ferris PolyMem, Burr Ridge, USA	Silver-impregnated polyurethane
Silverlon	Argentum Medical, Chicago, USA	Silver nylon fabric
SilvaSorb	AcryMed Company, Beaverton, USA	Silver absorbent wound dressing
Tegaderm Ag Mesh	3M Company, St. Paul, USA	Silver sulfate on mesh dressing
Urgotul SSD	Westons Internet, Sussex, UK	Hydrocolloid polyester net

The efficacy of a silver-coating in endotracheal tubes to prevent Ventilator-associated pneumonia (VAP) was studied by Kollef [68]. Two silver-coated tubes were tested against two uncoated tubes. One is commercially available – Agento® IC – and is coated with Ag^+ ions microdispersed in a proprietary hydrophilic polymer [69]. The other was under investigation, and consisted of a standard endotracheal tube coated in silver sulfadizine and polyurethane. Both silver-coated tubes were put through *in vitro* testing in a preclinical study, and the commercially available tube was put through a clinical study.

The *in vitro* studies showed a lack of bacterial colonization on both silver-coated tubes. The commercially available silver-coated tube showed a statistically-significant reduced incidence of VAP in the clinical study, with a relative risk reduction of 35.9%.

The Modular Universal Tumour and Revision System Silver (MUTARS®Silver) developed by Implantcast GmbH is a CE certified modular orthopaedic reconstructive endoprosthetic (megaprosthesis) and has been used in Europe for the treatment of osseus defects [70]. While reviewing existing literature for this thesis, the MUTARS®Silver implant system was the only silver-based orthopaedic implant that was found to be commercially available. The megaprosthesis consists of a silver-coating applied to a titanium-vanadium implant, to which an additional layer of gold is applied. The inherent potential difference between the two metals precipitates a release of Ag^+ ions into the periprosthetic tissue. Figure 2.3(a) shows the MUTARS®Silver megaendoprosthesis used in proximal femur replacement surgery. Figure 2.3(b) shows an x-ray of the megaendoprosthesis post-implantation.

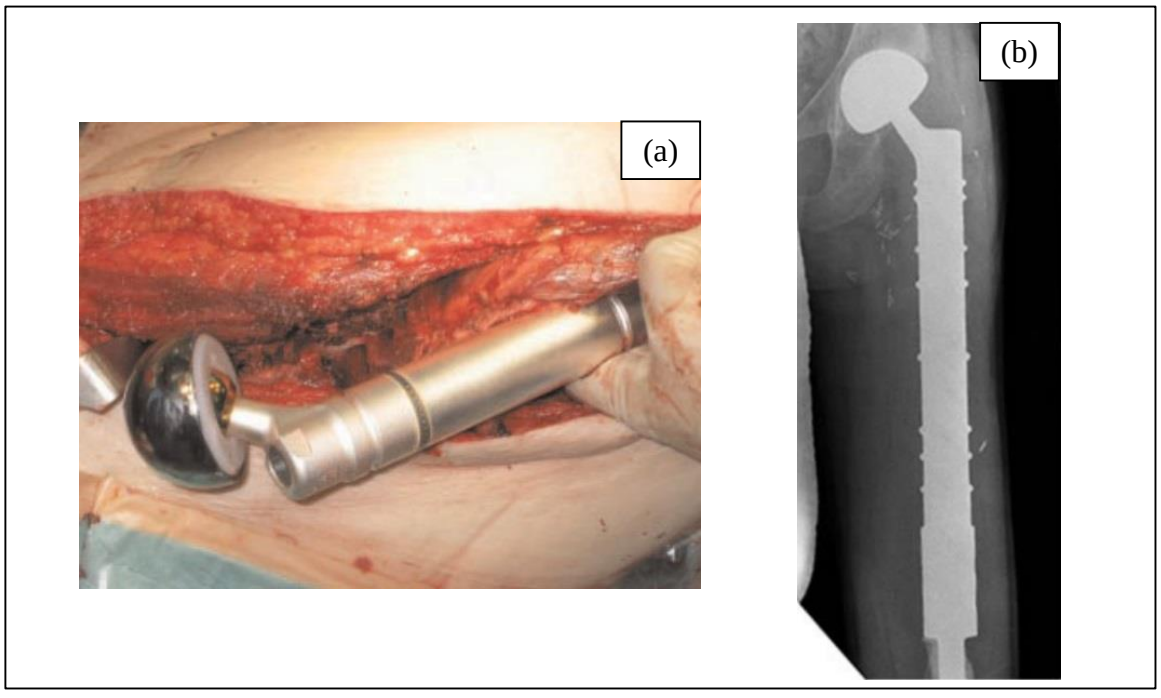

Figure 2.3(a) MUTARS®Silver silver-coated proximal femur replacement with a bipolar cup, and (b) post-operative x-ray of the megaendoprosthesis [72]

Gosheger et al tested the MUTARS® megaprosthesis in a rabbit model [71]. The study concluded that the MUTARS® megaprosthesis resulted in reduced infection rates without toxicological side effects, with the silver-coated megaprosthesis group reporting a 7% infection rate as opposed to the titanium group's 47%. Hardes et al tested the same system in human patients with bone sarcoma [72]. The infection rate was assessed over a period of 5 years. It was found that the incidence of infection in patients with the silver-coated megaprosthesis was 5.9% as compared to 17.6% in patients with the uncoated titanium implants. 38.5% of patients in the titanium group underwent post-infection amputation, while none of the patients in the silver group had to undergo amputation.

The devices discussed in this review so far have shown some of the different methods used for Ag^+ ion delivery, and the effectiveness of these against bacterial infections. There are examples of devices which use Ag-NPs liberated from a substrate [39] [73], Ag^+ ions liberated in an aqueous or colloidal solution [39] [74], and Ag^+ ions liberated through metal potential difference [71] [72]. However, the release of Ag^+ ions in these devices cannot be easily controlled and measured. This is a matter of concern, as it is known that there are recommended threshold concentrations for silver beyond which cytotoxic effects are seen [27]. Hence, a system in which the release and concentration of Ag^+ ions can be measured and controlled is necessary.

2.5 Iontophoretic Silver-based Antibacterial Implants

Spadaro et al tested the effect of LIDC passed through electrodes made of silver, gold, platinum, stainless-steel and copper on the growth of four bacterial species [23]. It was found that silver, even at very low currents (0.4 - 4 μA), had a very pronounced bacteriostatic effect. Furthermore, the concentration of silver in the medium was far less than expected. Further research by Berger et al found that electrically generated Ag^+ ions had a significantly lower Minimum Inhibitory Concentration (MIC) against bacteria than silver sulfadiazine, without any unfavorable effects on mammalian cells [75]. Becker et al and Webster et al both tested the efficacy of electrically generated Ag^+ ions against

chronic osteomyelitis with success [76] [77]. This research laid the foundation for silver-based electrically-activated antibacterial medical devices.

Raad et al tested this system by designing a silver iontophoretic catheter (SIC) prototype. A catheter with electrically charged silver wires wrapped around it was compared *in vitro* and *in vivo* with a catheter coated with chlorhexidine and silver sulfadiazine (CH/SS). It was found that the SIC retained its antibacterial activity past 30 days, while the antibacterial activity of the CH/SS-coated catheter reduced significantly. The *in vivo* tests in a rabbit model showed the SIC was safe and more effective at preventing *S. aureus* than the CH/SS-coated catheter [78].

Fuller et al re-examined the results of Spadaro et al's research and further characterized the iontophoretic antibacterial system by identifying the parameters affecting the antibacterial performance of the system [24]. Eight different metals – silver, copper, gold, titanium, nickel, zinc, cadmium and stainless steel (AISI 316L) – were used as electrodes (both cathode and anode) in this study. These were tested on seven different microbial species – *S. aureus, Enterococcus faecalis,* MRSA, *E. coli, P. aeruginosa, Proteus mirabilis and Cadida albicans* – at different levels of current, anode-cathode separation, and anode surface area. Cadmium, copper and silver were the only metals which demonstrated notable antimicrobial properties. However, copper was found to be effective only against Gram-positive species. In the absence of current, cadmium demonstrated the best antimicrobial efficacy. However, cadmium cannot be used in medical applications as it is known to show significant *in vivo* cytotoxicity [79] [80]. In the presence of a low current (0-20 μA), silver demonstrated the best antimicrobial efficacy. Furthermore, silver is less toxic than cadmium. Titanium and stainless steel, the contemporary materials in orthopaedic implant applications, showed no antimicrobial effects even with electrical activation. Hence, Fuller et al noted silver to be the optimal metal to be used for antimicrobial applications in an LIDC-activated system configuration. Following this, the system using silver electrodes was also tested *in vivo* in a rat model with some success [25].

The silver-based iontophoretic antibacterial system has several advantages over the other silver-based antibacterial systems discussed earlier in this chapter, with respect to orthopaedic implants. This system uses pure metallic silver rather than silver complexes, ensuring the Ag^+ ion is the only reactive species which evolves. Ag-NPs and other silver complexes, on the other hand, may potentially produce toxic byproducts due to the presence of a substrate (in the case of NPs) or other reactive species. The release of Ag^+ ions from pure metallic silver in an electrically activated setup is independent of environmental considerations. The quantity of Ag^+ ions can be easily controlled according to Faraday's law [24]. As a result of this, the prescribed cytotoxic limits can be adhered to with comparative ease.

Prior research in LIDC-based antimicrobial devices has always used the same metal for both electrodes. However, Fuller et al [24] observed inhibition zones only around the anode, and found that varying the surface area of the cathode did not significantly affect the area of these zones. In essence, there appeared to be no dependence of antibacterial efficacy on cathode-related design parameters. Therefore, keeping in mind the need for a non-antibiotic based antibacterial system which controllably releases bactericidal species while minimizing exposure to toxic substances, there exists sufficient scope and motivation to evaluate a silver-based iontophoretic antibacterial system which uses non-silver cathode materials.

2.6 Chapter Summary

Due to its antimicrobial properties, silver has been used in medicinal applications for centuries. In more recent times, it has been found that the release of Ag^+ ions is responsible for silver's antibacterial properties. Ag^+ ions attack bacterial cells in a multimodal manner, due to which the evolution of resistant bacteria is highly unlikely, making it ideal for medical applications. Although silver has been in use for topical antibacterial applications for decades, in recent years, many medical devices such as silver-coated catheters and endotracheal tubes have become commercially available.

These devices release Ag^+ ions by a variety of mechanisms like nanosilver liberation from a substrate, ionic liberation from aqueous or colloidal solutions, and ionic liberation through metal potential difference. However, it is difficult to regulate the release of Ag^+ ions from these products. This raises potential health concerns, as overexposure to silver is known to have adverse effects, the least of which is argyria, and the direst being damage to the nervous system, loss of motor function and cellular necrosis. The use of LIDC to release Ag^+ ions from pure metallic silver has shown promising results in the inhibition of bacterial growth, and gives a method by which the release of the Ag^+ ions can be easily controlled while also avoiding the formation of toxic byproducts. To further reduce exposure to silver, a multi-metal system is proposed which substitutes non-essential silver components with non-toxic and biocompatible materials like titanium and stainless steel, which are already commonly used in orthopaedic devices.

CHAPTER 3: METHODOLOGY AND EXPERIMENTATION

3.1 System Design

The purpose of the experimental setup described in this chapter is to apply a low intensity direct current (LIDC) between two metallic electrodes embedded within a bacterial growth medium in order to release metal ions to kill bacterial cells. Fuller et al [24] had originally configured and characterized this system design using eight different metals, and found silver to be the safest and most effective. The electrically activated system essentially follows the principle of oligodynamic iontophoresis [81]. The potential difference applied by the battery across the electrodes causes the release of Ag^+ ions from the anode. The electrodes are embedded in a growth medium inoculated with bacteria which itself acts as an electrolyte, promoting migration of Ag^+ ions between the electrodes. Due to the net negative charge on the bacterial cells, [82] the positively charged Ag^+ ions bind with the bacterial cells, causing cell death in a multi-modal manner as described in Chapter 2.

Fuller et al tested this system using electrode pairs made of the same metal (e.g., silver anode-silver cathode) in each metal testing configuration. Since there is no release of metal ions from the cathode, it is theorized that there is no dependence of the antibacterial action on the material of the cathode. In addition, no inhibition zones were formed around the cathodes. Furthermore, it was also found that there is no dependence of the antibacterial action on the surface area of the cathode and the electrode separation distance. Although silver demonstrated the optimal antibacterial efficacy, this result was only obtained for the silver-silver configuration; no data exists on the effect of these parameters in a system using dissimilar metals as electrodes. This research, therefore, aims to determine by means of a statistical empirical design if the choice of cathode material, cathode surface area and the separation between dissimilar electrodes will significantly affect the antibacterial efficacy of the electrically activated system. These experiments will be performed using *S. aureus* and *E. coli* as bacterial inoculants as they

are the commonly prevalent microorganisms in orthopaedic infections. Due to time and financial constraints, a three-factor statistical empirical design is conducted using the Gram-positive *S. aureus* alone, while a validation study to confirm the effect of cathode material uses Gram-negative *E. coli.* The results for *S. aureus* have been given priority as it is responsible for nearly 60% of nosocomial infections [83]. Furthermore, Gram-positive bacterial species are harder to kill than gram-negative species due to the presence of a thicker peptidoglycan layer on the cell wall [84] [85]. Fuller et al confirmed this, obtaining better results against *E. coli* than *S. aureus* [24]. This highlights the critical requirement for experimentation on the latter.

The experiments in this thesis test the efficacy of the system originally enumerated by Fuller et al using dissimilar metals as electrodes in the following three anode-cathode configurations:

- Silver-Silver (Ag-Ag)
- Silver-Titanium (Ag-Ti)
- Silver-Stainless Steel (Ag-SS)

The experimental system design consists of metal electrodes inserted diametrically oppositely into Mueller-Hinton agar, and connected to the terminals of a battery through a series of resistors in order to deliver the desired current. Since one of the objectives of this study is to test the effect of the electrode separation on antibacterial efficacy, it is necessary to control the distance between the two electrodes in the bacterial medium. As the dimensions of the agar plates are fixed, the electrodes themselves would be required to be moved until the desired separation is achieved. This could be done in either of two ways.

1. The electrodes could simply be moved until the desired separation is achieved. However, this would require the exposed ends of the copper connecting wires

which are wrapped around the ends of the electrodes to come into contact with the bacterial growth medium. This was undesirable as it would interfere with the results of the experiment.

2. The ends of the electrodes could be left protruding outside the agar plates, and instead, excess lengths of electrode material could be used until the electrodes are at the desired separation. However, this would not yield accurate results since the quantity of Ag^+ ions released is dependent on the surface area of the electrodes in contact with the bacterial medium.

This problem is remedied by the use of an insulating Polyfluorotetraethylene (PTFE) material to prevent the copper connecting wires on the ends of the electrodes from coming into contact with the agar. Additionally, the insulating PTFE is also used to manipulate the lengths of the electrodes in contact with the agar as well as the electrode separation. Figure 3.1 shows a schematic representation of the experimental setup.

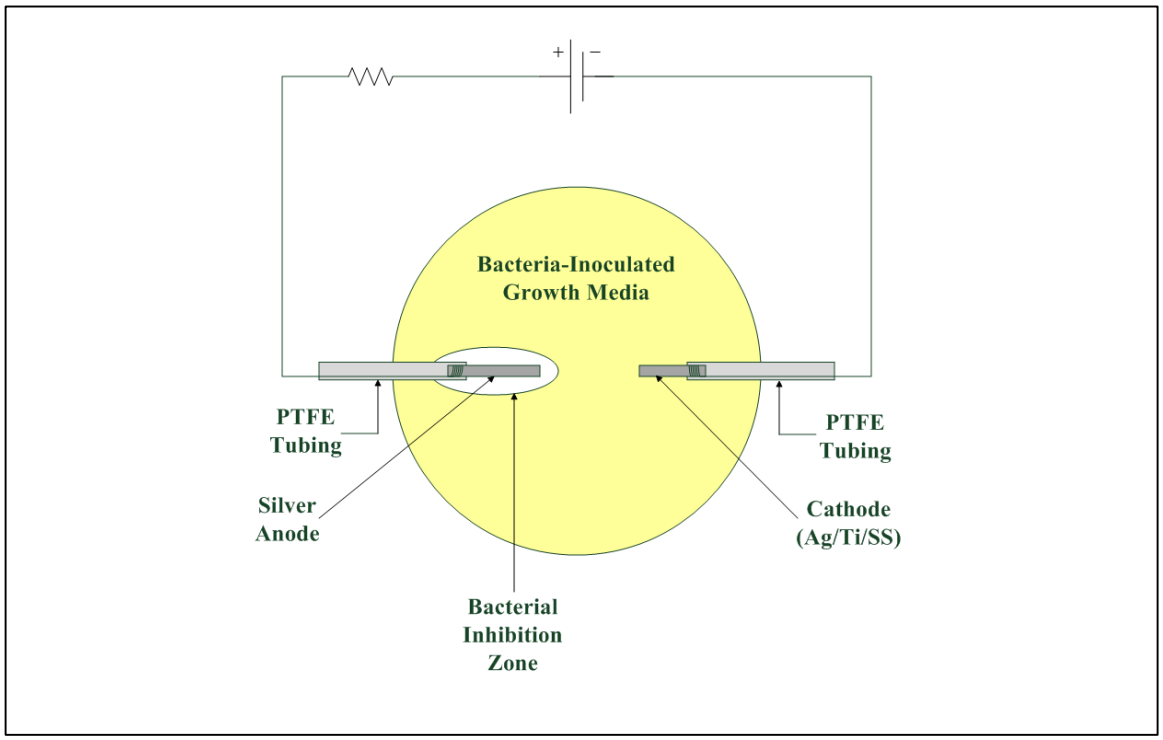

Figure 3.1 Schematic Representation of Experimental Setup

3.2 Testing Methodology

3.2.1 Testing Setup

The first step in the process of setting up the experiments was the preparation of the electrodes. Using a ruler, the active anode length (L) of 20 mm silver wire (Ø 1 mm) was measured and marked using a marker. An excess 3 mm was measured to have enough room to connect the enameled copper connecting wire to the electrode and apply the PTFE tubing (AWG I.D. Size No. 24). The cathode surface area was varied by varying the active cathode length (l) (Ø 1 mm). Similarly, the required length of cathode material (including the excess 3 mm) was measured, marked, and cut.

Next, approximately 100 mm of enameled copper connecting wires (Ø 0.2 mm) were cut. The ends of the enameled copper wire were exposed by briefly introducing them into the flame of a Bunsen burner. One exposed end of each wire was wound tightly around the 3 mm section of the electrode. The other end was left free for the time being. Subsequently, 40-50 mm of PTFE shrink tubing was cut for each electrode. The free end of the enameled copper wire was threaded through an open end of the shrink tubing and drawn out of the other end until the edge of the tubing lined up with the measured marking on the electrode. It is important for the edge of the shrink tubing to correctly align with the marking to ensure that the correct surface area of the electrode is exposed. It is also important to ensure that the wound end of the copper wire does not protrude past the edge of the shrink tubing beyond the 3 mm marking. Following that, the electrode assembly with the shrink tubing and copper wire was placed near the heating coil of a commercially available hair-dryer using forceps and exposed to a stream of heated air for 1.5-2 minutes to shrink the PTFE tubing around the electrode and copper wire to hold them in place. By visual inspection, it was ensured that the tubing had not torn and had shrunk tightly over the electrode-connector joint. Figure 3.2 shows the three sample electrode assemblies consisting of the metal electrode with the enameled copper wire

wound around the end and covered with the PTFE shrink tubing. The electrodes shown are an Ag anode (L = 20 mm), a Ti cathode (l = 20 mm), and a SS cathode (l = 10 mm).

The next step was the preparation of the agar plates. Initially, attempts were made to insert the electrodes into pre-filled and solidified agar plates. However, this involved multiple complications. Since maneuvering the electrodes deep into the plate was accomplished by holding and pushing one end of the shrink tubing, which is not sufficiently rigid, the tip of the electrodes often did not reach the desired position. Additionally, the process of inserting the electrode far enough into the plate caused tears in the agar over the testing interval, rendering results from those particular samples futile.

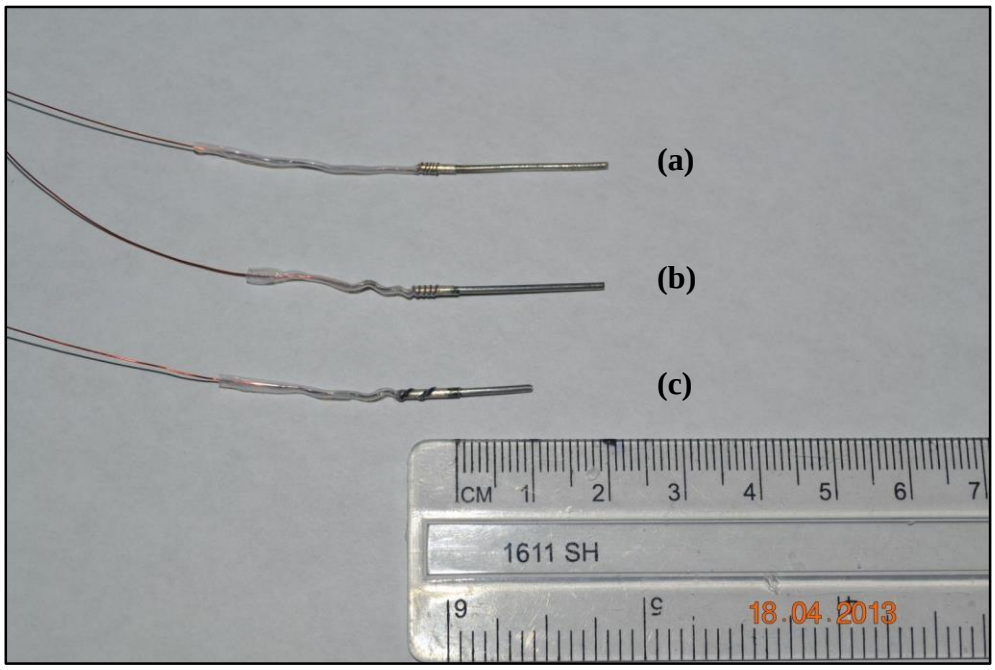

Figure 3.2 Electrode assemblies: (a) Ag anode, *L* = 20 mm (b) SS cathode, *l* = 20 mm (c) SS cathode *l* = 10 mm

Hence, the procedure was revised to pour molten agar into the plates after setting the electrode assemblies in their respective positions. In terms of the actual setup, the first step was to punch holes in the petridishes on diametrically opposite locations in order to insert the electrode assemblies. These holes were punched (Ø 2-3 mm) by heating the

sharp, thin tip of a small pair of scissors and gently pressing them into the wall of the petridish at the pre-marked site of the electrodes. Then, the electrode assemblies were slid into position through the holes. The desired electrode separation was measured using a ruler and the electrode assemblies were held in position using scotch tape. The position of the tips of the electrodes was marked with a marker to maintain positional consistency. Figure 3.3 shows the electrodes held in position with scotch tape before pouring molten agar into the plate.

In order to ensure that the molten agar does not leak through the holes made for the electrode assemblies, it is necessary to seal the holes. This was done by pouring melted wax onto the holes and waiting for it to solidify. This also held the electrode assemblies firmly in their desired positions.

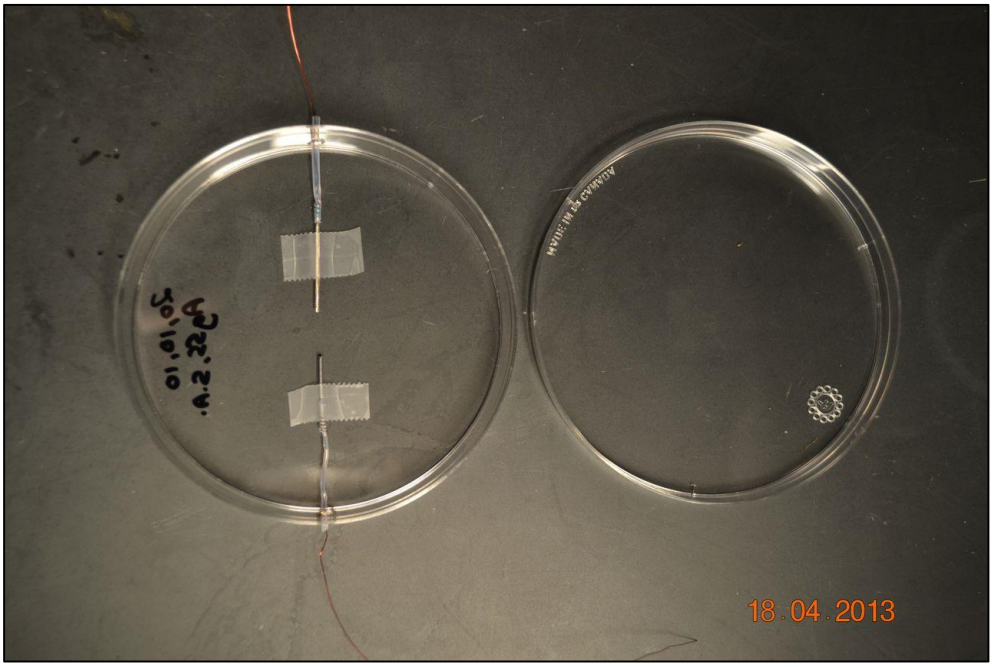

Figure 3.3 Electrodes held in position using scotch tape

The final step was the preparation of the Mueller-Hinton Agar. 1 liter of agar requires 39g of Mueller-Hinton agar powder. For this study, 500 ml is sufficient. Hence, 19.5g of Mueller-Hinton agar powder was weighed and poured into a bottle containing 500 ml of

distilled water. The bottle was closed, shaken well, and autoclaved for 30 minutes with a loose lid. On completion of the autoclave process, the bottle was held in a water bath at 60°C for 30 minutes. Finally, the scotch tape holding the electrode assemblies in place was removed, and the molten agar was poured into the petridish over the electrode assemblies. Bubbles in the agar were removed by applying the Bunsen burner at low heat to the surface of the agar. The agar plates were allowed to sit for 15 minutes to cool and solidify. The agar plates are now ready to be inoculated with bacteria, connected to the power circuit and incubated for 24 hours to start the actual testing. Figure 3.4 shows the prepared agar plates with electrodes inserted.

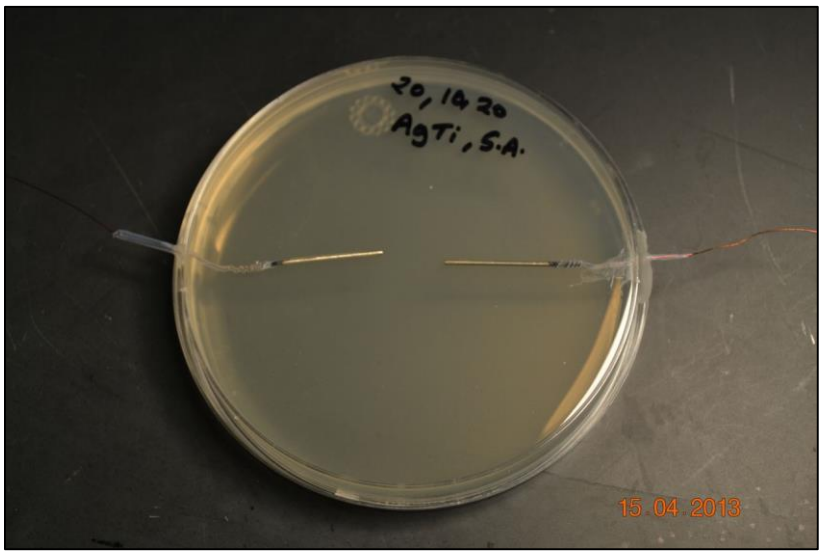

Figure 3.4 Prepared agar plate with electrodes inserted and held in place with wax. On the left is the anode (Ag) and on the right is the cathode (Ti, *l* = 20 mm), with 10 mm of electrode separation.

Table 3.1 lists the functions, technical specifications and suppliers of materials used in the experimental setup described.

Table 3.2 lists the system parameters that were kept constant throughout the experiments, and their levels.

Table 3.3 summarizes the electrode configurations and the levels of the system parameters being tested.

Table 3.1 List of Materials, Functions, Specifications and Suppliers

Material	Function	Specifications	Manufacturer/Supplier
Ag Wire	Anode, Cathode	99.99% Purity Temper Annealed Ø 1 mm	Advent Research Materials Ltd. (Oxford, UK)
Ti Wire	Cathode	99.6% purity Temper Annealed Ø 1 mm	Advent Research Materials Ltd. (Oxford, UK)
SS Wire	Cathode	AISI304L (Fe/Cr18/Ni10) Temper Annealed Ø 1 mm	Advent Research Materials Ltd. (Oxford, UK)
PTFE Heat Shrink Tubing	Insulating Material	AWG Size No. 24 (I.D.)	Zeus Inc. (Orangeburg, USA)
Batteries	Power Source	1.5 V * 4 (AA size Duracell) = 6 V	RadioShack (Cary, USA)
Resistors	Current Delivery	220 kΩ * 2 (in series) = 440 kΩ (delivering 15 μA)	RadioShack (Cary, USA)
Copper Wire	Conduction	Enameled, Ø 0.2 mm	Rowan Cable Products Ltd. (Hertfordshire, UK)
Breadboard	Power Circuit	2 1/8” Modular	RadioShack (Cary, USA)
Mueller-Hinton Agar	Bacterial Growth Medium	Dehydrated Culture Media (Ref: R454802)	Remel Microbiology Products (Waltham, USA)

Table 3.2 System Constant Parameters and Values

System Parameter	Value
Current (μA)	15
Voltage (V)	6 (1.5 V*4 cells)
Resistance (kΩ)	440 (2*220 kΩ in series)
Silver Anode Length (mm)	20
Silver Anode Diameter (mm)	1
Cathode (Ag/Ti/SS) Diameter (mm)	1
Incubation Time	24 hours
Incubation Temperature	37°C

Table 3.3 Electrode Configurations and Levels for experimental setup

Bacterial Species	*S. aureus*	*E. coli*
Configurations (Anode-Cathode)	Ag-Ag, Ag-Ti, Ag-SS	Ag-Ag, Ag-Ti, Ag-SS
Levels of Electrode Separation (mm)	10, 20, 40	20
Levels of Cathode Length (mm)	10, 20	10

3.2.2 Bacterial Preparation and Inoculation Protocol

The bacterial inoculants used for this experiment were ATCC cultures of *S. aureus* (ATCC 25213) and *E. coli* (MG1655), grown overnight on Mueller-Hinton Agar plates. The desired starting inoculant concentration was in the order of 10^7 cfu/ml. The inoculant was prepared in 0.7% Phosphate Buffered Saline (PBS). Two 5 ml tubes and two 1 ml cubic vials were used. One of the 5 ml tubes was marked "original" and the other as "dilute", while the cubic vials are marked "control" and "test". 3 ml of PBS was pipetted into the *original* tube, and 1 ml into the *control* vial. A needle loop was used to scrape off bacterial colonies (~10 for *S. aureus*, ~6 for *E. coli*) from the culture plate that was then mixed into the PBS in the *original* tube. The tube was placed on the vortex mixer until the bacteria uniformly mixed into the solution. 1 ml of bacterial solution was pipetted into the test vial. The OD 600 spectrophotometer was set to $\lambda = 600$ nm. The control vial was placed in the OD 600 and set to "Auto Zero", and the test vial was then placed in it. The OD 600 reading should ideally be ~0.2-0.4 indicating a concentration of 10^8 cfu/ml. 2 ml of the original solution was then pipetted into the dilute tube, and 0.2 ml of PBS added to dilute the solution to 10^7 cfu/ml. The inoculant was then applied to the agar plates by pipetting 0.1 ml of bacterial solution on to the agar top surface and swabbing evenly over the surface in 3 directions. The electrode assembly in the plate was then connected to the power circuit and incubated at 37°C for 24 hours to start the actual testing. Figure 3.5 shows the complete setup with the agar plates inoculated with bacteria connected to the power circuit.

The testing setup preparation and experiments were performed in the Medical Implants and Tissue Engineering (MITE) Lab (Department of Industrial and Systems Engineering) and the Orndorff Microbiology Lab (College of Veterinary Medicine Research Building) at NC State University, Raleigh, NC.

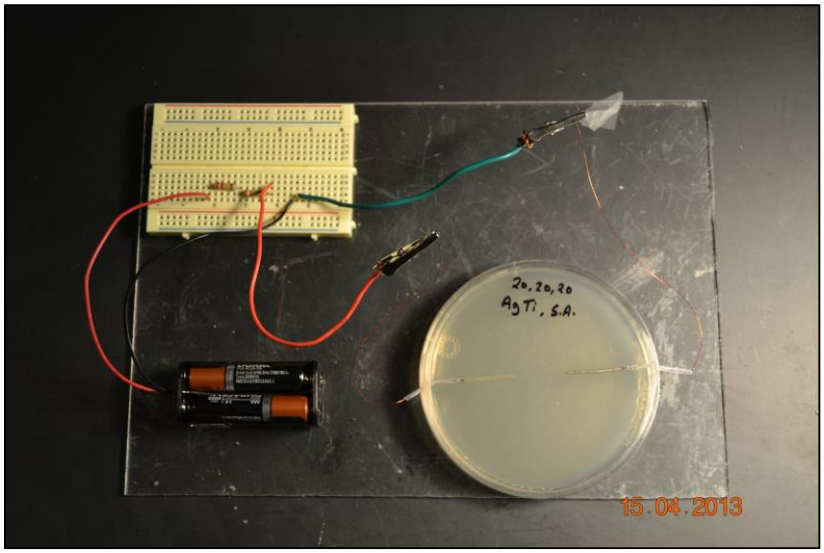

Figure 3.5 Complete Experimental Setup: Ag anode, Ti cathode (*l* = 20 mm) and 20 mm electrode separation distance, connected to the power circuit and inoculated with *S. aureus*

3.3 Statistical Empirical Design: Testing with *S. aureus*

The experiments were performed for three anode-cathode configurations, Ag-Ag, Ag-Ti, and Ag-SS. Each electrode configuration was tested at two levels of cathode length (*l*), which were 10 mm and 20 mm. Each configuration at each level of cathode length was tested at three levels of electrode separation, which were 10 mm, 20 mm, and 40 mm. One replication set in the empirical design is summarized in Table 3.4. The complete empirical design consisted of three sets of replications, with two samples being tested for each system configuration level within each replication. Hence, the total number of individual experimental setups tested was:

(3 electrode configurations) * (2 levels of cathode length) * (3 levels of electrode separation) *

(2 samples per plate) * (3 replications)

= **108**

Table 3.4 Summary of the system configurations in a single replication of the Empirical Design for testing with *S. aureus*

Electrode Configuration	**Ag - Ag**		**Ag - Ti**		**Ag - SS**	
Cathode Length (mm)	**10**	**20**	**10**	**20**	**10**	**20**
Electrode Separation (mm)	10	10	10	10	10	10
	20	20	20	20	20	20
	40	40	40	40	40	40

The objective of the study – to determine if the cathode material, electrode separation and cathode surface area have a significant effect on the system's antibacterial efficacy – was achieved by performing an Analysis of Variance (ANOVA) on the results obtained from the experiments.

3.4 Validation Study: Testing with *E. coli*

In order to verify that the same results were observed against Gram-negative bacterial species, testing on *E. coli* was performed after the experimentation on *S. aureus* was concluded. No observable effect was found to be caused by the cathode length and electrode separation distance in the experiments on *S. aureus* (results and discussion in Chapter 4), and hence *E. coli* was tested at only one level of cathode length and one level of electrode separation distance, over three electrode configurations. One replication of the validation study is summarized in Table 3.5. The validation study consisted of three sets of replications, with two samples being tested for each system configuration level within each replication. Hence, the total number of individual experimental setups tested was:

(3 electrode configurations) * (1 level of cathode length) * (1 level of electrode separation) * (2 samples per plate) * (3 replications) = **18**

Table 3.5 Summary of the system configurations in a single replication of the Validation Study for testing with *E. coli*

Electrode Configuration	**Ag - Ag**	**Ag - Ti**	**Ag - SS**
Cathode Length (mm)	10	10	10
Electrode Separation (mm)	20	20	20

The objective of the study – to determine if the cathode material has a significant effect on the system's antibacterial efficacy – was achieved by performing an ANOVA on the results obtained from the experiments.

3.5 Chapter Summary

Previous research applied the principle of oligodynamic iontophoresis to killing bacterial cells by the application of LIDC between silver electrodes embedded in a bacterial growth medium. This system was however, tested only using the same metal as both the anode and the cathode. As the release of metal ions to kill bacteria follows the principle of electrolysis, no metal ions are released from the cathode. Hence, keeping in mind the need to reduce exposure to silver due to its cytotoxic effects, an alternate system design has been proposed in which the cathode is replaced with a dissimilar metal. Titanium and stainless steel are commonly used in orthopaedic implants, and hence these materials are proposed as the cathodes in the alternate design. Three anode-cathode configurations – Ag-Ag, Ag-Ti, and Ag-SS – were tested for antibacterial efficacy using a statistical empirical design against *S. aureus* and *E. coli*. Protocols were developed to carry out the experiments at the specified system parameters. The tests on *S. aureus* were carried out at

two levels of cathode length and two levels of electrode separation distance, while the validation study on *E. coli* was performed at one level of both Cathode Length and Electrode Separation. Three replications were carried out, with two samples at each parameter level. The antibacterial efficacy was expressed in terms of the area of the bacterial inhibition zones around the anodes. An ANOVA was performed on the inhibition zone areas from the experiments to determine if cathode material, Cathode Length and Electrode Separation have a statistically significant effect on the antibacterial efficacy.

CHAPTER 4: RESULTS AND ANALYSIS

4.1 Experimental Results

The empirical design and protocols were outlined in Chapter 3. Each of the 3 electrode configurations, i.e. Ag-Ag, Ag-Ti, and Ag-SS, were tested at cathode lengths (*l*) of 10 mm and 20 mm, and Electrode Separation Distances (ESDs) of 10 mm, 20 mm, and 40 mm (Table 3.4). A voltage of 6 V was applied between the electrodes to generate a system current of 15 µA in each plate for 24 hours at 37°C. The experiment was run for three replications in order to get a sufficiently large pool of data.

After incubation for 24 hours, the plates were taken out of the incubator to measure the antibacterial efficacy of the system by measuring the dimensions of the bacterial inhibition zones formed around the anodes. The length of the inhibition zone was measured along the longitudinal axis of the anode, and its width measured perpendicular to the length. Due to the sometimes irregular shape of the inhibition zones, the width was taken as an average of three measurements along the length. Theoretically, the inhibition zone is a combined shape of a rectangle and two semicircles. In practice, inhibition zones often don't display such a regular shape, and hence the area is approximated. Figure 4.1 shows the different shapes evaluated for Inhibition Zone Area calculations.

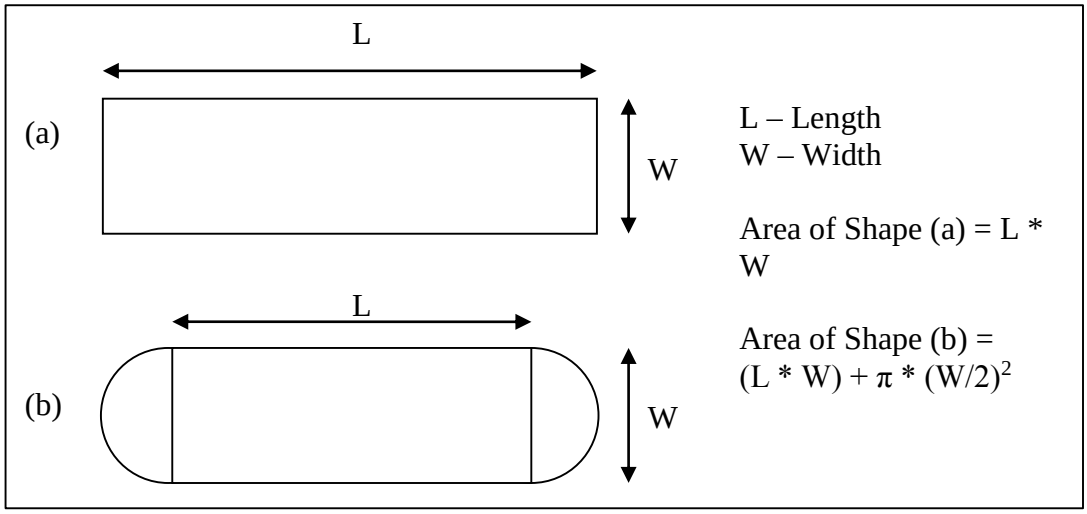

Figure 4.1 Inhibition Zone Shape-Based Area Calculations

The Inhibition Zone Areas were calculated both as rectangular areas as well as the combined areas of a rectangle and two semicircles. It was found that the area calculated as a rectangle gave a better approximation, as this bore a closer resemblance to the actual inhibition zone shapes. In the plate shown in Figure 4.2 (a) and (b), the Inhibition Zone areas calculated by the two methods were found to be within 8.8% of each other, and hence the rectangular area was taken as a reasonable approximation. Figure 4.2 shows how the length and width of the inhibition zones were measured. Tables 4.1 and 4.2 shows the measured inhibition zone areas for *S. aureus* and *E. coli* respectively. These areas are the average of 2 samples of each electrode configuration at each level of Cathode Length and ESD.

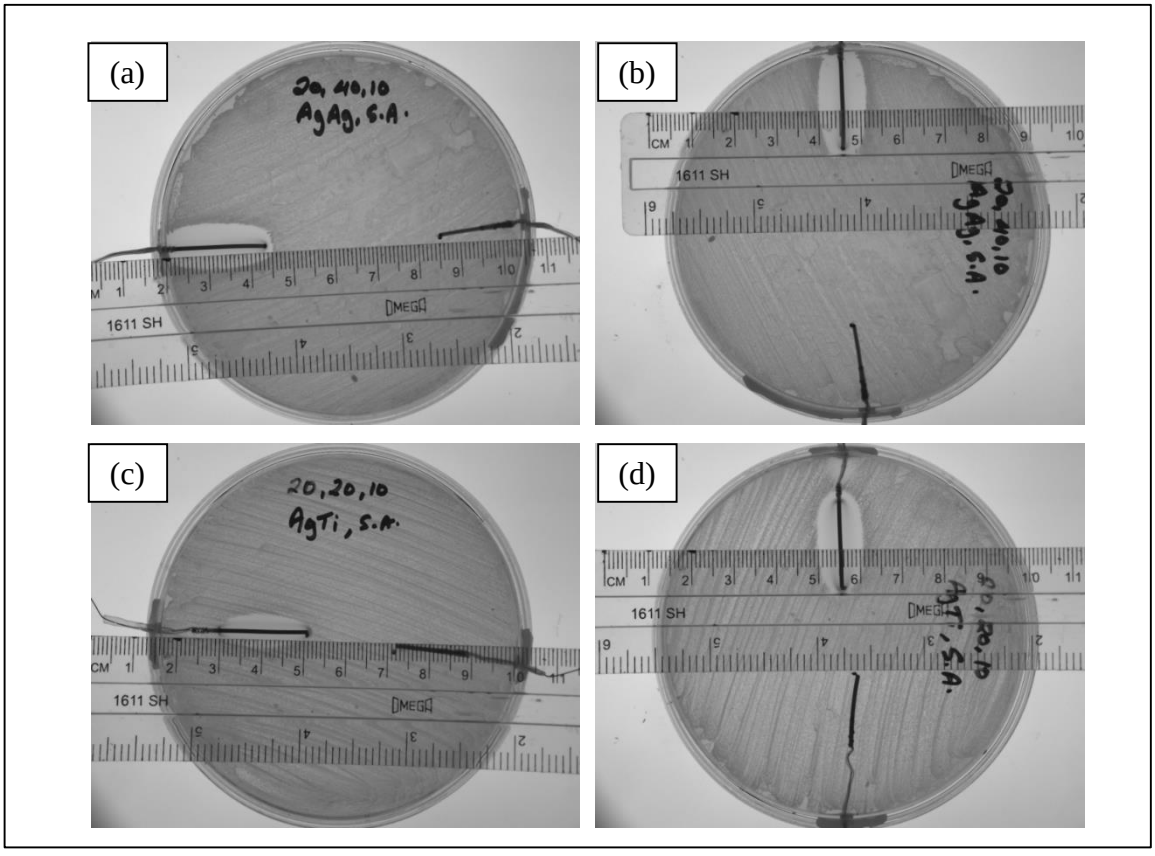

Figure 4.2 Length and Width Measurement of Inhibition Zone Area: (a) Length of Ag-Ag (*l* = 10 mm, ESD = 40 mm), (b) Width of Ag-Ag (*l* = 10 mm, ESD = 40 mm), (c) Length of Ag-Ti (*l* = 10 mm, ESD = 20 mm), and (d) Width of Ag-Ti (*l* = 10 mm, ESD = 40 mm)

Table 4.1 Inhibition Zone Areas (in mm^2) for *S. aureus*

Replication	Electrode Configuration	Cathode Length (mm)	Inhibition Zone Area (mm^2)		
			ESD (mm)		
			10	20	40
1	Ag-Ag	10	286.00	292.67	330.38
		20	306.58	293.76	317.11
	Ag-Ti	10	230.38	184.00	233.00
		20	229.13	146.93	173.20
	Ag-SS	10	222.63	206.75	249.46
		20	180.96	231.84	265.42
2	Ag-Ag	10	193.50	188.93	265.68
		20	223.22	168.43	166.60
	Ag-Ti	10	179.43	193.34	213.36
		20	218.50	191.06	188.00
	Ag-SS	10	136.60	132.74	153.00
		20	216.85	138.21	137.83
3	Ag-Ag	10	164.50	171.36	207.26
		20	159.00	170.60	174.32
	Ag-Ti	10	175.43	196.02	210.71
		20	182.25	153.82	172.26
	Ag-SS	10	231.75	258.91	236.51
		20	265.70	218.39	281.72

Table 4.2 Inhibition Zone Areas (in mm^2) for *E. coli*

Replication	Electrode Configuration	Inhibition Zone Area (mm^2)
		***l* = 10 mm, ESD = 20 mm**
1	Ag-Ag	150.100
	Ag-Ti	149.100
	Ag-SS	223.920
2	Ag-Ag	242.580
	Ag-Ti	227.425
	Ag-SS	175.440
3	Ag-Ag	139.900
	Ag-Ti	161.485
	Ag-SS	136.395

All observations from experiments run on *S. aureus* are listed in Appendix A. All experiments from experiments run on *E. coli* are listed in Appendix B.

4.2 Statistical Analysis

4.2.1 Statistical Analysis of Results for *S. aureus*

The results obtained from the experiments on *S. aureus* were modeled as a three-factor statistical design. 2 samples of each experimental setup were run, and the average of these 2 samples was taken as an observation. Hence, from 108 individual experiments, $N = 54$ observations were made across $\alpha\beta\gamma = 18$ treatment combinations (3 Electrode Configurations * 2 Cathode Lengths * 3 ESDs) over 3 replications.

The factors, levels, and representative variables are summarized in Table 4.3

Table 4.3 Three-Factor Statistical Design Parameters

Factor	Level	Variable
Electrode Configuration	Ag-Ag	α_1
	Ag-Ti	α_2
	Ag-SS	α_3
Cathode Length (mm)	20	β_1
	10	β_2
ESD (mm)	40	γ_1
	20	γ_2
	10	γ_3

These factors were modeled using a three-way ANOVA model with the response variable Y_{ijkl} representing the Inhibition Zone area.

$$Y_{ijkl} = \mu + \alpha_i + \beta_j + \gamma_k + (\alpha\beta)_{ij} + (\alpha\gamma)_{ik} + (\beta\gamma)_{jk} + (\alpha\beta\gamma)_{ijk} + \varepsilon_{ijkl} \quad \text{...(Eq. 1)}$$

$$i = 1, 2, 3;\ j = 1, 2;\ k = 1, 2, 3;\ l = 1, 2, 3;$$

$$\varepsilon_{ijkl} \sim iid\ N(0, \sigma^2)$$

The ANOVA analysis was performed using the statistical software RStudio© (Version 0.97.449, RStudio Inc., Vienna, Austria). Figure 4.3 shows a screen capture of the ANOVA output from RStudio.

```
Console ~/
> anova(lm(Area~Configuration*Cathode.Length*ESD, New))
Analysis of Variance Table

Response: Area
                                Df Sum Sq Mean Sq F value Pr(>F)
Configuration                    2  10308  5154.1  1.9716 0.1519
Cathode.Length                   1    552   551.9  0.2111 0.6482
ESD                              1   1694  1694.1  0.6481 0.4253
Configuration:Cathode.Length     2   2343  1171.5  0.4482 0.6418
Configuration:ESD                2    880   439.9  0.1683 0.8457
Cathode.Length:ESD               1   3604  3604.4  1.3788 0.2469
Configuration:Cathode.Length:ESD 2   1546   773.0  0.2957 0.7455
Residuals                       42 109793  2614.1
>
```

Figure 4.3 ANOVA Table from RStudio Output for *S. aureus*

RStudio carries out Analysis of Variance at a 95% confidence level by default. From the figure above, it can be noted that the p-values of all factors and interactions are > 0.05.

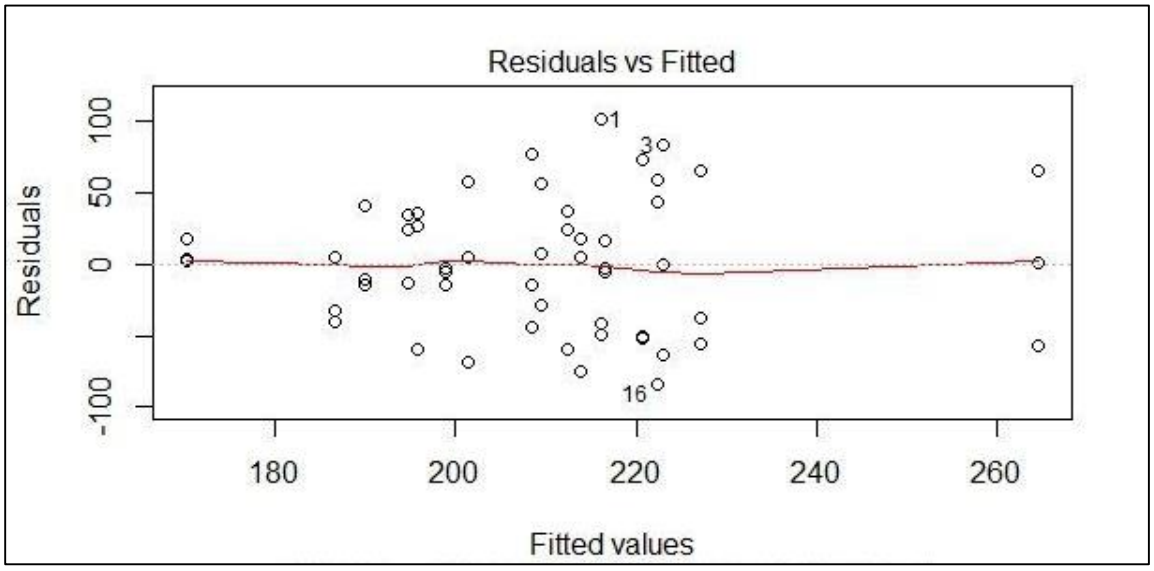

Figure 4.4 Residuals vs. Fitted Values Plot for *S. aureus*

In order to check the validity of the model in Equation 1, the residual plot, normal probability plot and the p-value of the ANOVA were examined. Figure 4.4 shows the

Residuals vs. Fitted Values plot. The plot shows a random pattern dispersed around the horizontal axis with no evidence of discernible trends, indicating the residuals are not correlated to the predicted response values.

Figure 4.5 shows the normal probability plot of the standardized residuals. It can be seen that the standardized residuals fit the linear pattern representing the idealized normally distributed data.

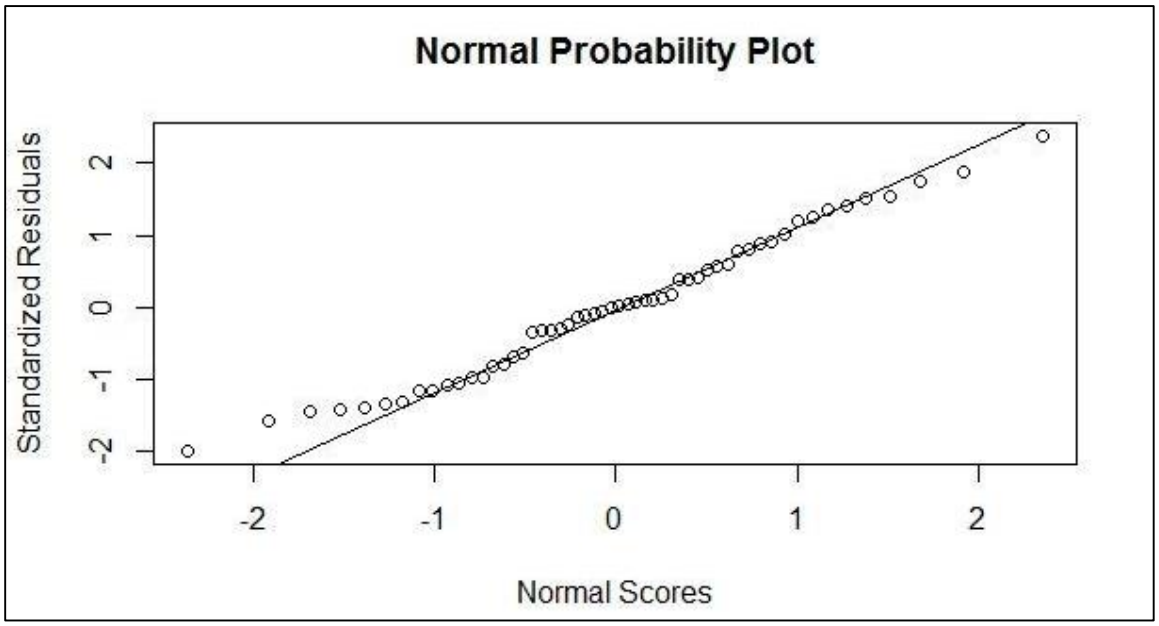

Figure 4.5 Normal Probability Plot of Residuals for *S. aureus*

Furthermore, the p-value from the RStudio summary of the linear model fit to the data (Figure 4.6) has a value of 0.7059. This proves the residual terms are normally distributed. Therefore, these observations i.e. the random distribution of residuals with no discernible trend, the linear pattern displayed by the normal probabilty plot of residuals, and the high p-value, confirm the validity of the adopted linear model.

```
Coefficients:
                                          Estimate Std. Error t value Pr(>|t|)
(Intercept)                             153.82083   80.84114   1.903   0.0639
ConfigurationAg-SS                       21.56067  114.32664   0.189   0.8513
ConfigurationAg-Ti                        5.41483  114.32664   0.047   0.9624
Cathode.Length                            3.57858    5.11284   0.700   0.4878
ESD                                       3.98349    3.05551   1.304   0.1994
ConfigurationAg-SS:Cathode.Length        -2.09362    7.23065  -0.290   0.7736
ConfigurationAg-Ti:Cathode.Length        -1.38962    7.23065  -0.192   0.8485
ConfigurationAg-SS:ESD                   -3.31029    4.32114  -0.766   0.4479
ConfigurationAg-Ti:ESD                   -1.39744    4.32114  -0.323   0.7480
Cathode.Length:ESD                       -0.21082    0.19325  -1.091   0.2815
ConfigurationAg-SS:Cathode.Length:ESD     0.19887    0.27329   0.728   0.4708
ConfigurationAg-Ti:Cathode.Length:ESD     0.04057    0.27329   0.148   0.8827
---
Signif. codes:  0 '***' 0.001 '**' 0.01 '*' 0.05 '.' 0.1 ' ' 1

Residual standard error: 51.13 on 42 degrees of freedom
Multiple R-squared:  0.1601, Adjusted R-squared:  -0.05988
F-statistic: 0.7278 on 11 and 42 DF,  p-value: 0.7059
```

Figure 4.6 RStudio Summary of Fitted Model for *S. aureus*

4.2.2 Statistical Analysis of Results for *E. coli*

The experiments on *E. coli* were performed after analysis of the results of the results of the experiments on *S. aureus.* As the p-values for all Cathode Length and ESD, as well their interactions, were found to be > 0.05, it was concluded that these two factors did not contribute significantly, and hence only the effect of cathode material was studied in the experiments on *E. coli.* The results obtained from the experiments were modeled as a single-factor statistical design. 2 samples of each experimental setup were run, and the average of these 2 samples was taken as an observation. Hence, from 18 individual experiments, $N = 9$ observations were made across $\alpha = 3$ treatments over 3 replications. Table 4.4 summarizes the factor, levels, and representative variables.

The response variable Y_{ij} represents the Inhibition Zone Area.

$$Y_{ij} = \mu + \alpha_i + \varepsilon_{ij} \quad \text{...(Eq. 2)}$$

$$i = 1, 2, 3$$

$$j = 1, 2, 3$$

$$\varepsilon_{ij} \sim iid\ N(0, \sigma^2)$$

Table 4.4 Single-Factor Statistical Design Parameters

Factor	Level	Variable
Electrode Configuration	Ag-Ag	α_1
	Ag-Ti	α_2
	Ag-SS	α_3

Figure 4.7 shows a screen capture of the ANOVA output from RStudio.

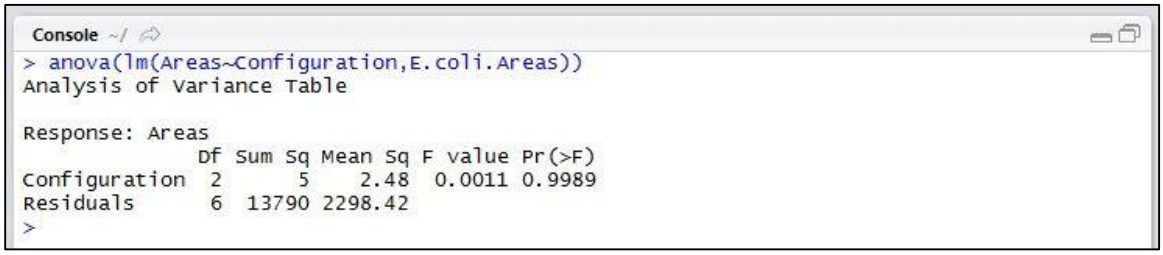

Figure 4.7 ANOVA Table from RStudio Output for *E. coli*

Analysis of Variance was carried out at a 95% confidence level. From the figure above, it can be noted that the p-values of the factor Configuration is > 0.05.

The linear model fitted to the data shows a high p-value of 0.9989. However, since the number of data points available is low, a check for model validity has not been performed. The results obtained for the validation study on *E. coli* indicate that the antibacterial efficacy of the iontophoretic antibacterial system against *E. coli* does not depend on the material of the cathode, but this cannot be stated to a statistical certainty without a larger sample size.

4.3 Discussion

The ANOVA of the Inhibition Zone Areas in both *S. aureus* and *E. coli* showed $p > 0.05$ for all factors and interactions. From this it is inferred that the Electrode Configuration, Cathode Length and ESD do not have a significant effect on the size of the Inhibition Zone in both Gram-positive and Gram-negative bacteria. Furthermore, there are no significant interactions between the three factors.

The lack of statistical significance of the cathode material in the design of the iontophoretic antibacterial system suggests that the assumption stated in Section 1.3 is correct; i.e. the choice of cathode material does not appear to affect the bactericidal efficacy of the system, and a different cathode material may be substituted instead of silver without compromising the system's ability to prevent bacterial infection. It has been found that Ti and SS are indeed suitable materials for use in this system. This is advantageous as both these metals are widely used in medical implants due to their favorable mechanical properties and biocompatibility.

The lack of statistical significance of the Cathode Length and ESD suggests the independence of the antibacterial efficacy of the system from cathode design parameters. Furthermore, the results show that there are no significant interactions between the choice of cathode material and cathode design parameters. This allows for iontophoresis-based antibacterial orthopaedic implant design to be unconstrained by cathodic surface area and spatial placement of the cathode. Cathode material can serve a dual-purpose in the design of an orthopaedic implant; Ti and SS are already in use as structural materials in orthopaedic implants, and can also be used as cathodic surfaces. This allows for the optimal utilization of materials in implant design.

Table 4.6 summarizes the average areas of the Inhibition Zones in *S. aureus* over three replications at each level of Cathode Length and ESD. Figure 4.8 shows their plot on a bar graph. Although no statistical significance has been found between the different configurations, some observations and recommendations may be made based on the

trends in the data. Additionally, these observations are prompted by the material properties of the cathode material. On the whole, the antibacterial performance of the Ag-Ag electrode configuration is marginally better than that of the other two electrode configurations. The next best performance is shown by the Ag-SS electrode configuration. Ag-Ti shows average inhibition zone area marginally less than the other two electrode configurations. It is desirable to limit the biological exposure to silver, but the Ag-Ag electrode configuration shows the best results. Hence, it may be appropriate to limit the application of the Ag-Ag electrode configuration to short-term implants where there is a high possibility of bacterial infection, for example in external fixators used to treat battlefield-inflicted orthopaedic trauma. Another potential application is in articulating spacers. Currently, these spacers are used to treat orthopaedic infections by implant removal, debridement and placement of an high dosage antibiotic-impregnated spacer [86]. These may be replaced with silver-based iontophoretic articulating spacers. As high concentrations of Ag^+ ions are required to eliminate deep-seated infections, and these are short-term devices, the Ag-Ag configuration may be used. Stainless steel has low cytotoxicity [62], and is also far cheaper than silver (Table 4.5). As the Ag-SS electrode configuration shows slightly lower antibacterial efficacy than the Ag-Ag electrode configuration, it may be used in short-term applications and temporary implants in an environment where the risk of bacterial infection may be controlled to a greater extent, such as external fixators used in the fixation of broken bones. The Ag-Ti electrode configuration showed the smallest inhibition zones. However, due to its biocompatibility and ability to osseointegrate [28], titanium is far more suitable for long-term implants like hip- and knee-joint replacements than silver and stainless steel. Hence, the Ag-Ti electrode configuration may be used in such applications in conjunction with prescription antibiotics to reduce the risk of infection. It should be noted that the factors studied in this research are not the only ones affecting antibacterial efficacy. Appropriately revising other critical parameters like the current, voltage and anode surface area can increase the antibacterial efficacy of the Ag-Ti configuration to similar levels as that of the Ag-Ag configuration.

Table 4.5 Prices of Silver, Titanium and Stainless Steel [87]

Metal	Silver	Titanium	Stainless Steel
Price (USD/lb)	567	6.5	0.995

Note: Silver price is converted from USD/Troy Oz. to USD/lb

While the Ag-Ag and Ag-Ti electrode configurations show the highest efficacy at l = 10, ESD = 40, the Ag-SS electrode configurations appears to be most efficient at l = 20 and ESD = 40. All three electrode configurations appear to show the worst antibacterial performance at l = 20 and ESD = 20. Although no statistical significance is attributed to the different Cathode Lengths and ESDs, the trends displayed in the data might provide valuable information pertinent to the design parameters of an iontophoretic antibacterial implant using the configurations described in these tests.

Table 4.6 Average Inhibition Zone Areas in *S. aureus* over three replications

		Average Inhibition Zone Area (mm^2)		
Electrode Configurations		**Ag-Ag**	**Ag-Ti**	**Ag-SS**
l = 10	ESD = 10	214.67	195.08	196.99
	ESD = 20	217.65	191.12	199.47
	ESD = 40	267.77	219.02	212.99
l = 20	ESD = 10	229.60	209.96	221.17
	ESD = 20	210.93	163.93	196.15
	ESD = 40	219.34	177.82	228.32

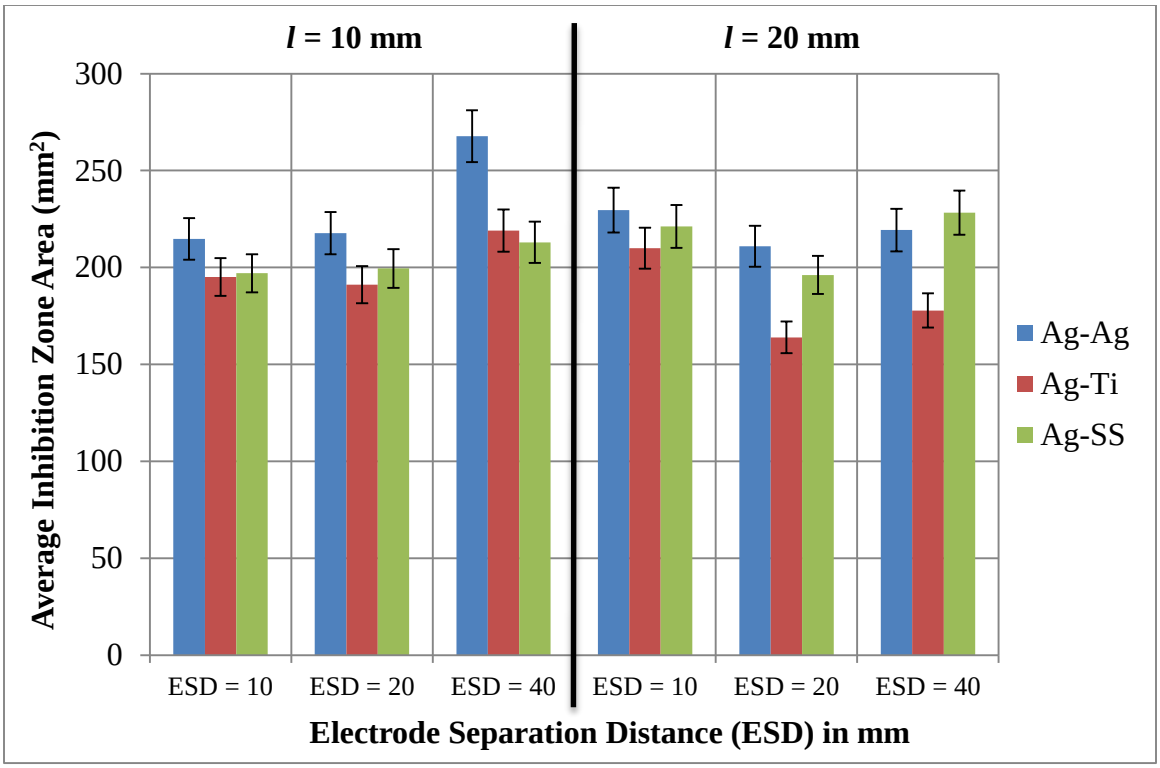

Figure 4.8 Average Inhibition Zone Areas for experiments on *S. aureus*

Table 4.7 and Figure 4.9 summarize the Average Inhibition Zone Areas for the three electrode configurations against *E. coli*. Due to the small sample size and the proximity of the average values to one another, no conclusions can be drawn on the comparative performance of the three electrode configurations. However, it can be concluded from the results of the validation study that titanium and stainless steel are viable cathode materials which will not compromise the efficacy of the iontophoretic antibacterial system.

Table 4.7 Average Inhibition Zone Areas in *E. coli* over three replications

	Average Inhibition Zone Area (mm^2)		
Electrode Configurations	**Ag-Ag**	**Ag-Ti**	**Ag-SS**
l = 10, ESD = 20	177.527	179.337	178.585

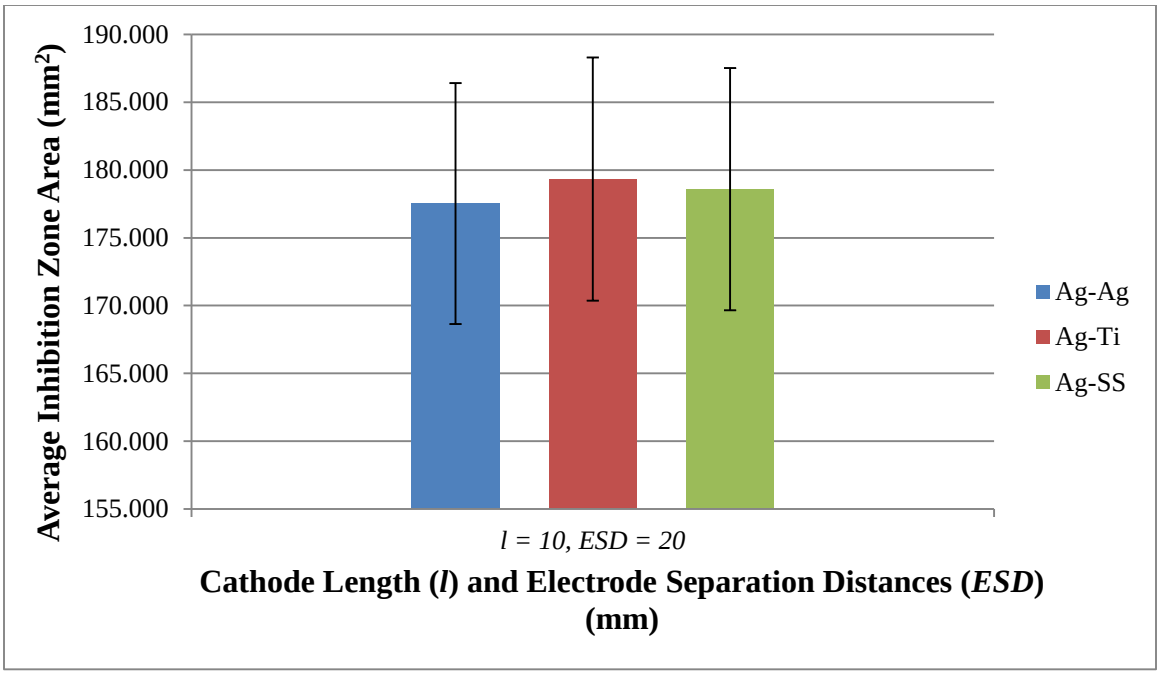

Figure 4.9 Average Inhibition Zone Areas for experiments on *E. coli*

4.4 Chapter Summary

The protocols and system parameters for the experiments carried out were described in Chapter 3. Once each set of experiments was performed, the results were noted in the form of the area of the inhibition zones formed around the anode. These areas were measured by measuring the length and width of the inhibition zones and finding the rectangular area. Statistical analysis of the results was performed by fitting statistical linear models to the data. For the *S. aureus* results, Configuration, Cathode Length and ESD were modeled as factors and Inhibition Zone Area as the response in a three-factor ANOVA. RStudio was used to perform an ANOVA of the model at 95% confidence level. None of the factors were found to have a significant effect on the Inhibition Zone Area. The results of the validation study of *E. coli* were modeled as a single-factor ANOVA with Configuration as a factor and Inhibition Zone Area as the response. No significant effect of cathode material on the Inhibition Zone area was noted. These results indicate that the cathode material may be substituted without affecting the antibacterial

efficacy of the system. As titanium and stainless steel are materials with a history of use in orthopaedic implants, and have favorable material properties, their use as cathode material is advantageous and has been proven effective by this study. Depending on the application, environment of use, and duration of implantation, the different configurations may be used in the design of an iontophoretic antibacterial orthopaedic implant device.

CHAPTER 5: CONCLUSIONS AND FUTURE WORK

5.1 Conclusions

The use of iontophoretic silver in the prophylaxis of bacterial infection in orthopaedic implants has been previously studied and characterized. The research presented in this document addresses the question of reducing exposure to silver in order to preclude the deleterious effects of its cytotoxicity without compromising antibacterial efficacy. This was done by replacing the silver cathode with two other metals widely used in medical devices, titanium and stainless steel. The choice of cathode metals is based on their biocompatibility, low cytotoxicity and favorable material properties.

By the use of statistically designed experiments, it has been found that there exists insufficient evidence to suggest that the antibacterial performance of devices with the proposed alternative cathode materials may be different from that of the original design consisting of silver cathodes. It has also been found that the cathode surface area and electrode separation distance do not affect the performance of the system. This allows the design of iontophoretic antibacterial implants to be unconstrained by cathode design parameters and spatial placement of the cathode material. Titanium and stainless steel can thus optimize the implant design, serving a dual purpose, as both structural materials and cathodic materials. The implications of these results are both medically and economically significant, as the cathode materials used are less cytotoxic, more biocompatible and less expensive than silver. Some potential applications of each proposed electrode configuration have been identified with the goal of striking a balance between reducing exposure to cytotoxic silver and exploiting its bactericidal properties.

The multi-metal iontophoretic antibacterial system has been tested against both *S. aureus* and *E. coli*. This has given data on the performance of the system against both Gram-positive and Gram-negative bacteria. Thus the choice of cathode material has been found to not significantly contribute to the antibacterial efficacy of the system against both kinds of bacterial species'.

The research presented in this documented characterized the performance of the multi-metal iontophoretic antibacterial orthopaedic implant system based on three factors: cathode material, cathode surface area, and electrode separation distance. Further characterization of this system is required to better understand the effect of other factors like anode surface area and level of current on the antibacterial efficacy. Fuller et al studied the effect of these factors on antibacterial efficacy for a system using similar metals, and found them to be of significant importance. But no such studies have been conducted on a system with dissimilar metals.

5.2 Future Work

The work enumerated in this thesis is based on the results obtained by Fuller et al. A new system configuration involving multi-metal electrodes has been proposed and evaluated for antibacterial efficacy. However, there is scope for a deeper characterization of the proposed system. Some directions for future work have been listed below.

1. Testing in a 3-Dimensional Setup

The experiments performed in this research were all carried out in petridishes; the bacterial inoculant was only applied on the top surface of the growth medium, and the bacterial inhibition was only studied in a two-dimensional setting. Although this setup simulates soft tissue, it is not possible to monitor the diffusion of ions in the medium in real-time. This prevents quantitative assessment of bacterial performance and ion release. It is necessary to perform studies using the same setup in a three-dimensional space, using a liquid growth medium like Tryptic Soy Broth (TSB) and so as to observe the volume of the three-dimensional inhibition regions.

2. Testing Against Different Bacterial Species

The bacterial species selected for this study were chosen due to their ubiquity and to reflect the performance of the system against Gram positive (*S. aureus*) and Gram negative (*E. coli*) species'. However, it is necessary to test the system against other

common bacterial species associated with orthopaedic infection like *Pseudomonas aeruginosa* and *Enterococcus faecalis*. More significantly, it is necessary to test the system against strains of bacteria like Methicillin-resistant *S. aureus* and Vancomycin-resistant *S. aureus*. Since this method of antibacterial action is intended to reduce the dependence on antibiotics, testing the efficacy of the system against these antibiotic-resistant strains is of great importance.

3. Testing for Varying Durations of Time

The tests in this study were all run for a period of 24 hours. The intended application of these devices, however, may vary between weeks to years. Certain potential applications of this system, like articulating antibacterial spacers, are used only for a few weeks, while applications like hip and knee implants are used for years. These considerations must be taken into account in the device design, and further characterization is required along these lines. Furthermore, it is necessary to study their long-term effectiveness i.e. to determine if antibacterial efficacy reduces over longer periods of time, if degradation of electrodes occurs etc.

4. Cytotoxicity Studies

The objective of this study was to reduce the amount of silver being used in the iontophoretic antibacterial system. However, this has only been done qualitatively – no assessment has been performed of the concentration of Ag^+ ions being released, and whether this falls within prescribed cytotoxic levels. It is therefore crucial to quantitatively model the diffusion of Ag^+ ions with respect to parameters like anode surface area and current applied. Furthermore, it is important to assess the cytotoxic effects of these ions on cells like osteoblasts and osteoclasts.

5. Dimensional Considerations

The experiments performed in this study were carried out using wires measured in mm for electrodes. However, to more accurately understand the behavior of these devices in

their intended environment, the components must be scaled up in size to more closely resemble the orthopaedic implants which they are intended to be used in, and tested in an appropriately dimensioned *in vitro* setting.

6. *In Vivo* Studies

Once the above mentioned tests have been performed in an *in vitro* setting, it is necessary to validate the model by testing it in an *in vivo* setting. Wysk et al. tested the iontophoretic antibacterial orthopaedic implant system in an osteomyelitic rat model [25]. The study helped to obtain a clearer picture of biological interactions, design considerations, and safety issues. It is, therefore necessary to carry out such *in vivo* studies on the system proposed in this thesis before it can be endorsed for commercialization.

7. Additional Results and their Implications

Some initial experiments which were run during the course of this study yielded interesting and potentially useful results. The experimental setup was similar to the other experiments described in this document – the anode and cathode were inserted from diametrically opposite sides of the petridish into the bacterial growth media. All system parameters were identical to the experiments described except for the anode and cathode surface areas – both the electrodes had an active length of 25 mm. It was observed that at this level of electrode length, for the Ag-Ag configuration, bacterial inhibition zones appeared not only around the anode, but around the cathode as well. No such cathodic inhibition zones were observed for the Ag-Ti configuration. A faint and very narrow inhibition zone appeared to exist around the cathode for the Ag-SS configuration. Figure 5.1 shows images of these experiments. A cathodic inhibition zone can clearly be seen for the Ag-Ag configuration. No cathodic inhibition zone is seen for the Ag-Ti configuration, and a faint cathodic inhibition zone is seen for the Ag-SS configuration. Three replications of this experiment were performed, with identical results in each replication.

This result was not obtained for any anode lengths less than 25 mm. It is unclear if the cathode length in the Ag-Ag configuration has a role to play in the appearance of the cathodic inhibition zone, as no tests were performed with anode length > 25 mm and cathode length < 25 mm. The implications of this result are significant, as it would be possible to design a device with an Ag-Ag configuration with high antibacterial efficacy due to the presence of two inhibition zones.

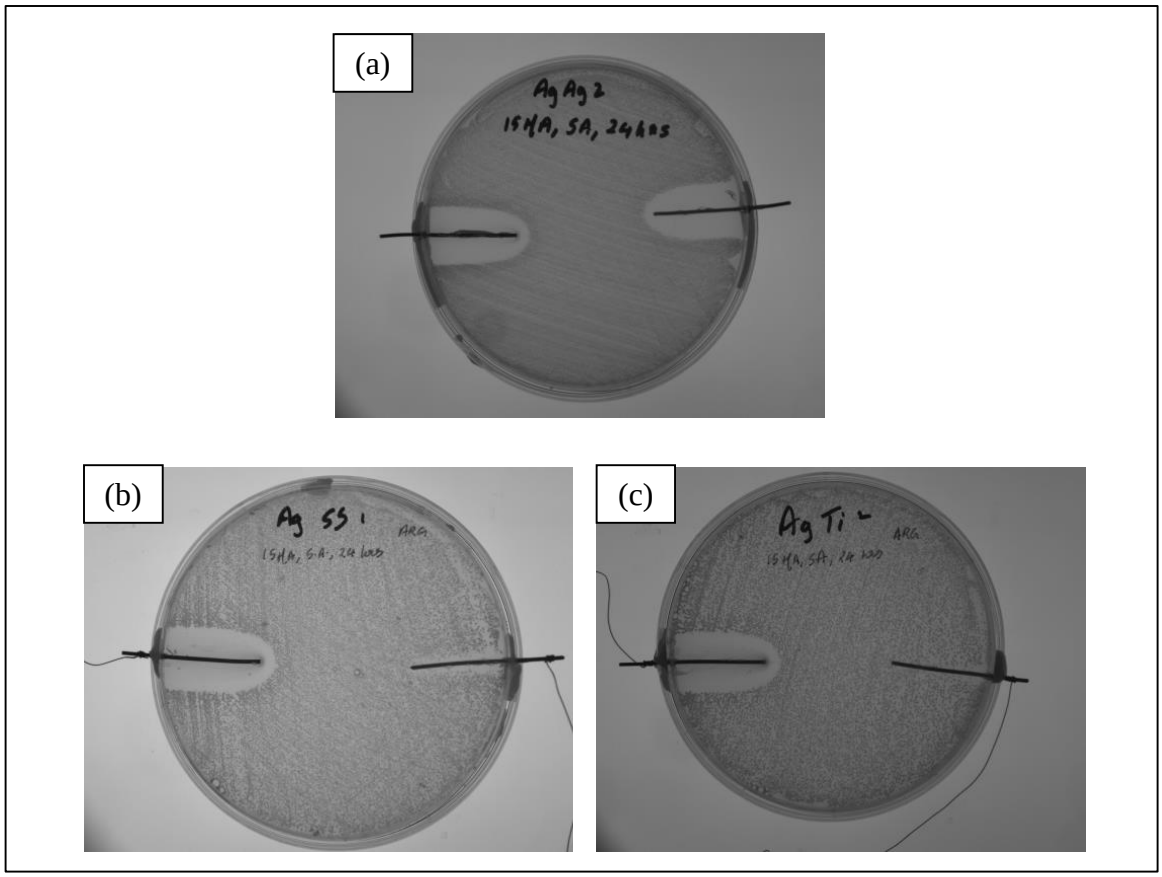

Figure 5.1 Inhibition Zones in experiments with 25 mm Anode and Cathode Lengths: (a) Configuration Ag-Ag with clear Inhibition Zones around both electrodes; (b) Configuration Ag-SS with faint Inhibition Zone around the cathode; and (c) Configuration Ag-Ti with no Inhibition Zone around the cathode.

However, as the cytotoxic effect of silver must be kept in mind, such a device would necessarily be usable only in temporary applications like articulating spacers and external

fixators for fracture fixation. Further experimentation is required to investigate this phenomenon and understand the reasons for its occurrence.

The results from these additional experiments performed are listed in Appendix C.

REFERENCES

[1] P. H. King and R. C. Fries, Design of Biomedical Devices and Systems, Taylor & Francis Group, 2009.

[2] Y. Holtzmann, "The U.S. Medical Device Industry in 2012: Challenges at Home and Abroad," *Medical Device and Diagnostic Industry*, 2012.

[3] R. Paddock and M. Hein, "International Trade Administration: A Bureau within the Department of Commerce," [Online]. Available: http://www.ita.doc.gov/td/health/outlook_05_medical.pdf. [Accessed 23 March 2013]

[4] A. Norton, "More Americans getting pacemakers," Reuters, 26 September 2012. [Online]. Available: http://www.reuters.com/article/2012/09/26/us-more-americans-getting-pacemakers-idUSBRE88P1LN20120926. [Accessed 23 March 2013]

[5] "National Center for Health Statistics: Inpatient Surgery FastStats," Center for Disease Control - National Center for Health Statistics, 16 May 2012. [Online]. Available: http://www.cdc.gov/nchs/fastats/insurg.htm. [Accessed 23 March 2013]

[6] S. Kurtz, K. Ong, E. Lau, F. Mowat and M. Halpern, "Projections of primary and revision hip and knee arthroplasty in the United States from 2005 to 2030," *The Journal of Bone & Joint Surgery*, vol. 89, no. 4, 2007.

[7] "Overview of Medical Device Regulation," U.S. Food and Drug Administration, 5 December 2012. [Online]. Available: http://www.fda.gov/MedicalDevices/DeviceRegulationandGuidance/Overview/GeneralandSpecialControls/default.htm. [Accessed 23 March 2013]

[8] C. F. van Eck, A. F. Chen, B. A. Klatt, J. D'Antonio and F. H. Fu, "The Classification of Implants: Class I, II, III," *Journal of Long-Term Effects of Medical Implants,* 2009.

[9] "Class II Special Controls Guidance Document: Hip Joint Metal/Polymer Constrained Cemented or Uncemented Prosthesis; Guidance for Industry and FDA," U.S. Food and Drug Administration, 30 April 2002. [Online]. Available: http://www.fda.gov/MedicalDevices/DeviceRegulationandGuidance/GuidanceDocuments/ucm072917.htm. [Accessed 23 March 2013]

[10] A. T. Fragomen and S. R. Rozbruch, "The Mechanics of External Fixation," *HSS Journal,* 2007.

[11] S. M. Perren, "Evolution of the Internal Fixation of Long Bone Fractures - The Scientific Basis of Biological Internal Fixation: Choosing a New Balance Between Stability and Biology," *The Journal of Bone & Joint Surgery,* 2002.

[12] K. C. Saikia, S. K. Bhuyan, T. D. Bhattacharya, M. Borgohain, P. Jitesh and F. Ahmed, "Internal fixation of fractures of both bones forearm: Comparison of locked compression and limited contact dynamic compression plate," *Veterinary and Comparative Orthopaedics and Traumatology,* vol. 45, no. 5, 2011.

[13] M. A. Catalado, N. Petrosillo, M. Cipriani, R. Cauda and E. Tacconelli, "Prosthetic joint infection: Recent developments in diagnosis and management," *Journal of Infection,* 2010.

[14] A. Trampuz and W. Zimmerli, "Diagnosis and treatment of infections associated with fracture-fixation devices," *Injury: International Journal of the Care of the Injured,* no. 37, 2006.

[15] C. Lavernia, D. J. Lee and V. H. Hernandez, "The Increasing Financial Burden of Knee Revision Surgery in the United States," *Clinical Orthopaedics & Related Research,* 2006.

[16] J. Barberan, "Management of infections of osteoarticular prosthesis," *Clinical Microbiology and Infection*, 2006.

[17] D. L. Cavanaugh, J. Berry, S. R. Yarboro and L. E. Dahners, "Better Prophylaxis Against Surgical Site Infection with Local as Well as Systemic Antibiotics," *The Journal of Bone and Joint Surgery,* vol. 91, no. 8, 2009.

[18] A. D. Russell and W. B. Hugo, Progress in Medicinal Chemistry, Elsevier Science B.V., 1994.

[19] B. S. Atiyeh, M. Costagliola, S. N. Hayek and S. A. Dibo, "Effect of silver on burn wound infection control and healing: Review of the literature," *Burns,* vol. 33, no. 2, 2007.

[20] M. Beattie and J. Taylor, "Silver alloy vs. uncoated urinary catheters: a systematic review of the literature," *Journal of Clinical Nursing*, vol. 20, no. 15-16, 2011.

[21] Xiao Li, Qiang Yuan, Li Wang, Liang Du and Lijing Deng, "Silver-coated endotracheal tube versus non-coated endotracheal tube for preventing ventilator-associated pneumonia among adults: A systematic review of randomized controlled trials," *Journal of Evidence-Based Medicine,* vol. 5, no. 1, 2012.

[22] A. Panacek, L. Kvitek, R. Prucek, M. Kolar, R. Vecerova, N. Pizurova, V. K. Sharma, T. Nevecna and R. Zboril, "Silver Colloid Nanoparticles: Synthesis, Characterization, and Their Antibacterial Activity," *The Journal of Physical Chemistry,* vol. 110, no. 33, 2006.

[23] J. A. Spadaro, T. J. Berger, S. D. Barranco, S. E. Chapin and R. O. Becker, "Antibacterial Effects of Silver Electrodes with Weak Direct Current," *Antimicrobial Agents and Chemotherapy,* vol. 6, no. 5, 1974.

[24] T. A. Fuller, R. A. Wysk, C. Charumani, M. Kennett, W. J. Sebastiennelli, R. Abrahams, R. A. Shirwaiker, R. C. Voigt and P. Royer, "Developing an engineered antimicrobial/prophylactic system using electrically activated bactericidal metals," *Journal of Materials Science: Materials in Medicine,* vol. 21, no. 7, 2010.

[25] R. A. Wysk, W. J. Sebastianelli, R. A. Shirwaiker, G. M. Bailey, C. Charumani, M. Kennett, A. Kaucher, R. Abrahams, T. A. Fuller, P. Royer, R. C. Voigt and P. H. Cohen, "Prophylactic Bactericidal Orthopedic Implants - Animal Testing Study," *Journal of Biomedical Science and Engineering,* vol. 3, no. 9, 2010.

[26] P. L. Drake and K. J. Hazelwood, "Exposure-Related Health Effects of Silver and Silver Compounds: A Review," vol. 49, no. 7, 2005.

[27] L. Kvitek, A. Panacek, R. Prucek, J. Soukupova, M. Vanickova, M. Kolar and R. Zboril, "Antibacterial activity and toxicity of silver - nanosilver versus ionic silver," *Journal of Physics: Conference Series,* vol. 304, no. 1, 2011.

[28] J. Emsley, Nature's Building Blocks: An A-Z Guide to the Elements, Oxford: Oxford University Press, 2001.

[29] J. W. Alexander, "History of the Medical Use of Silver," in *25th Annual Meeting of the Surgical Infection Society*, Miami Beach, FL, 2005.

[30] H. J. Klasen, "Historical review of the use of silver in the treatment of burns. I. Early uses," *Burns,* vol. 26, no. 2, 2000.

[31] N. J. Logie, "Treatment of Burns at Tobruk," *The Lancet*, vol. 1, no. 6246, 1943.

[32] C. A. Moyer, L. Brentano, D. L. Gravens, H. W. Margraf and W. W. Monafo, "Treatment of large human burns with 0.5% silver nitrate solution," *Archives of Surgery*, vol. 90, no. 6, 1965.

[33] J. Lee, K. Kim, W. S. Sung, J. G. Kim and D. G. Lee, "The Silver Nanoparticle (Nano-Ag): a New Model for Antifungal Agents," 2010. [Online]. Available: http://www.intechopen.com/books/silver-nanoparticles/thesilver-nanoparticle-nano-ag-a-new-model-for-antifungal-agents. [Accessed 23 March 2013]

[34] "Medline Plus," U.S. National Library of Medicine, 01 February 2009. [Online]. Available: http://www.nlm.nih.gov/medlineplus/druginfo/meds/a682598.html. [Accessed 09 April 2013].

[35] A. B. Lansdown, "Silver in health care: antimicrobial effects and safety in use.," *Current Problems in Dermatology*, vol. 33, 2006.

[36] Y. Zhou, Y. Kong, S. Kundu, J. D. Cirillo and H. Liang, "Antibacterial activities of gold and silver nanoparticles against Escherichia coli and bacillus Calmette-Guérin," *Journal of Nanobiotechnology*, vol. 10, no. 19, 2012.

[37] I. Sondi and B. Salopek-Sondi, "Silver nanoparticles as antimicrobial agent: a case study on E. coli as a model for Gram-negative bacteria," *Journal of Colloid and Interface Science*, vol. 275, no. 1, 2004.

[38] "Acticoat Antimicrobial Barrier Dressing," Smith & Nephew, [Online]. Available: http://www.smith-nephew.com/key-products/advanced-wound-management/acticoat/. [Accessed 16 April 2013].

[39] S. Silver, L. T. Phung and G. Silver, "Silver as biocides in burn and wound dressings and bacterial resistance to silver compounds," *Journal of Industrial Microbiology and Biotechnology,* vol. 33, 2006.

[40] M. Rai, A. Yadav and A. Gade, "Silver nanoparticles as a new generation of antimicrobials," *Biotechnology Advances,* vol. 27, no. 1, 2009.

[41] W. J. Schreurs and H. Rosenberg, "Effect of silver ions on transport and retention of phosphate by Escherichia coli," *Journal of Bacteriology,* vol. 152, no. 1, 1982.

[42] W. Ghandour, J. A. Hubbard, J. Deistung, M. N. Hughes and R. K. Poole, "The uptake of silver ions by Escherichia coli K12: toxic effects and interaction with copper ions," *Applied Microbiology and Technology,* vol. 28, 1988.

[43] A. Lansdown, "Silver I: its antibacterial properties and mechanism of action," *Journal of Wound Care,* vol. 11, no. 4.

[44] P. Dibrov, J. Dzioba, K. K. Gosink and C. C. Hase, "Chemiosmotic Mechanism of Antimicrobial Activity of Ag+ in Vibrio cholerae," *Antimicrobial Agents and Chemotherapy,* vol. 46, no. 8, 2002.

[45] Q. L. Feng, J. Wu, G. Q. Chen, F. Z. Cui, T. N. Kim and J. O. Kim, "A mechanistic study of the antibacterial effect of silver ions on Escherichia coli and Staphylococcus aureus," *Journal of Biomedical Materials Research,* vol. 52, no. 4, 2000.

[46] M. C. Fung and D. L. Bowen, "Silver products for medical indications: risk-benefit assessment," *Journal of Toxicology - Clinical Toxicology,* vol. 34, no. 1, 1996.

[47] A. Wadhera and M. Fung, "Systemic argyria associated with ingestion of colloidal

silver," *Dermatology Online Journal,* vol. 11, no. 1, 2005.

[48] W. R. Hill, "Argyria: The Pharmocology of Silver," *Southern Medical Journal,* vol. 34, no. 3, 1941.

[49] "Agency for Toxic Substances & Disease Registry," U.S. Centers for Disease Control and Prevention, 03 March 2011. [Online]. Available: http://www.atsdr.cdc.gov/phs/phs.asp?id=537&tid=97. [Accessed 09 April 2013].

[50] J. Liu, Z. Wang, F. D. Liu, A. B. Kane and R. H. Hurt, "Chemical Transformations of Nanosilver in Biological Environments," *ACS Nano,* vol. 6, no. 11, 2012.

[51] J. Rungby, "An experimental study on silver in the nervous system and on aspects of its general cellular toxicity.," *Danish Medical Bulletin,* vol. 37, no. 5, 1990.

[52] N. R. Panyala, E. M. Pena-Mendez and J. Havel, "Silver or silver nanoparticles: a hazardous threat to the environment and human health?," *Journal of Applied Biomedicine,* vol. 6, 2008.

[53] "Integrated Risk Information System," U.S. Environmental Protection Agency, 09 August 2012. [Online]. Available: http://www.epa.gov/iris/subst/0099.htm#reforal. [Accessed 11 April 2013].

[54] C. Marambio-Jones and E. M. Hoek, "A review of the antibacterial effects of silver nanomaterials and potential implications for human health and the environment," *Journal of Nanoparticle Research,* vol. 12, 2010.

[55] G. Danscher and L. J. Locht, "In vivo liberation of silver ions from metallic silver surfaces," *Histochemistry and Cell Biology,* vol. 133, 2010.

[56] J. S. Hayes and R. G. Richards, "The use of titanium and stainless steel in fracture

fixation," *Expert Review of Medical Devices,* vol. 7, no. 6, 2010.

[57] "Natural-Knee II Modular CoCr Cemented Tibial Baseplate," Zimmer, [Online]. Available: http://www.zimmer.com/en-US/hcp/knee/product/natural-knee-ii-modular-cocr-baseplate.jspx. [Accessed 11 April 2013].

[58] "Titanium Implant System," Hermann-Medizintechnik, [Online]. Available: http://www.hermann-medizintechnik.ch/centixcms/en/shop/suchen/8.html. [Accessed 11 April 2013].

[59] "Stryker Xia Stainless Steel Implant," Stryker, [Online]. Available: http://www.stryker.com/en-us/products/Spine/Thoracolumbar/Xia3Implant/XiaStainlessSteel/index.htm. [Accessed 11 April 2013].

[60] "HipLOC Compression Hip Screw System," Biomet, [Online]. Available: http://www.biomet.com/trauma/products.cfm?pdid=4&majcid=29&prodid=318. [Accessed 11 April 2013].

[61] "SKY Implant System - Titanium," Bredent Medical, [Online]. Available: http://www.bredent-medical.com/en/medical/product-information-v2/20010/. [Accessed 11 April 2013].

[62] T. Santonen, H. Stockmann-Juvala and A. Zitting, "Finnish Institute of Occupational Health," 2010. [Online]. Available: http://www.ttl.fi/en/publications/Electronic_publications/Documents/Stainless_steel.pdf. [Accessed 09 April 2013].

[63] I. Gotman, "Characteristics of metals used in implants," *Journal of Endourology,* vol. 11, no. 6, 1997.

[64] M. E. Hiro, Y. N. Pierpont, F. Ko, T. E. Wright, M. C. Robson and W. G. Payne, "Comparative Evaluation of Silver-Containing Antimicrobial Dressings on In Vitro and In Vivo Processes of Wound Healing," *Eplasty*, vol. 12, no. 48, 2012.

[65] J. J. Castellano, S. M. Shafii, F. Ko, G. Donate, T. E. Wright, R. J. Mannari, W. G. Payne, D. J. Smith and M. C. Robson, "Comparative evaluation of silver-containing antimicrobial dressings and drugs," *International Wound Journal*, vol. 4, no. 2, 2007.

[66] S. Thomas and P. McCubbin, "A comparison of the antimicrobial effects of four silver-containing dressings on three organisms," *Journal of Wound Care*, vol. 12, no. 3, 2003.

[67] E. Ulkur, O. Oncul, H. Karagoz, E. Yeniz and B. Celikoz, "Comparison of silver-coated dressing (Acticoat™), chlorhexidine acetate 0.5% (Bactigrass®), and fusidic acid 2% (Fucidin®) for topical antibacterial effect in methicillin-resistant Staphylococci-contaminated, full-skin thickness rat burn wounds," *Burns*, vol. 31, no. 7, 2005.

[68] M. Kollef, "Preventive Strategies in VAP: Focus on Silver-Coated Endotracheal Tubes," in *T.F. Moriarty et al. (eds.), Biomaterials Associated Infection: Immunological Aspects and Antimicrobial Strategies*, New York, Springer Science+Business Media, 2013, pp. 531-555.

[69] "Agento I.C. Endotracheal Tube," Bard Medical, [Online]. Available: http://www.bardmedical.com/AGENTOI.C.EndotrachealTube. [Accessed 16 April 2013].

[70] "MUTARS (Modular Universal Tumor And Revision System)," Implantcast GmbH, [Online]. Available:

http://www.implantcast.info/index.php?option=com_content&view=category&layout=blog&id=1&Itemid=57&lang=en. [Accessed 11 April 2013].

[71] G. Gosheger, J. Hardes, H. Ahrens, A. Streitburger, H. Buerger, M. Erren, A. Gunsel, F. H. Kemper, W. Winkelmann and C. von Eiff, "Silver-coated megaendoprostheses in a rabbit model—an analysis of the infection rate and toxicological side effects," *Biomaterials,* vol. 25, no. 24, 2004.

[72] J. Hardes, C. Von Eiff, A. Streitbuerger, M. Balke, T. Budny, M. P. Henrichs, G. Hauschild and H. Ahrens, "Reduction of Periprosthetic Infection With Silver-Coated Megaprostheses in Patients With Bone Sarcoma," *Journal of Surgical Oncology,* vol. 101, 2010.

[73] K. Dunn and V. Edwards-Jones, "The role of Acticoat with nanocrystalline silver in the management of burns," *Burns,* vol. 30, no. 1, 2004.

[74] B. Jorgensen, P. Price, K. E. Andersen, F. Gottrup, N. Bech-Thomsen, E. Scanlon, R. Kirsner, H. Rheinen, J. Roed-Petersen, M. Romanelli, G. Jemec, D. J. Leaper, M. H. Neumann, J. Veraart, S. Coerper, R. H. Agerslev, S. H. Bendz, J. R. Larsen and R. G. Sibbald, "The silver-releasing foam dressing, Contreet Foam, promotes faster healing of critically colonised venuos leg ulcers: a randomized, controlled trial," *International Wound Journal,* vol. 2, no. 1, 2005.

[75] T. J. Berger, J. A. Spadaro, S. E. Chapin and R. O. Becker, "Electrically Generated Silver Ions: Quantitative Effects on Bacterial and Mammalian Cells," *Antimicrobial Agents and Chemotherapy,* vol. 9, no. 2, 1976.

[76] R. O. Becker and J. A. Spadaro, "Treatment of Orthopaedic Infections with Electrically Generated Silver Ions," *The Journal of Bone and Joint Surgery,* vol. 60, no. 7, 1978.

[77] D. A. Webster, J. A. Spadaro, R. O. Becker and S. Kramer, "Silver Anode Treatment of Chronic Osteomyelitis," *Clinical Orthopaedics & Related Research,* vol. 161, 1981.

[78] I. Raad, R. Hachem, A. Zermeno, L. Stephens and G. P. Bodey, "Silver Iontophoretic Catheter: A Prototype of a Long-Term Anti-infective Vascular Access Device," *The Journal of Infectious Diseases,* vol. 173, 1996.

[79] A. Dubreuil, G. Bouley and C. Boudene, "In vitro cytotoxicity of cadmium microparticles for rabbit pulmonary alveolar macrophages.," *Scandinavian Journal of Work, Environment and Health,* vol. 5, no. 3, 1979.

[80] L. M. Latinwo, V. L. Badisa, C. O. Odewumi, C. O. Ikediobi, R. B. Badisa, A. Brooks-Walter, A. T. Lambert and J. Nwoga, "Comparative evaluation of cytotoxicity of cadmium in rat liver cells cultured in serum-containing medium and commercially available serum-free medium.," *International Journal of Molecular Medicine,* vol. 22, no. 1, 2008.

[81] D. Anderson, F. L. Milder and B. D. Weitzner, "Iontophoretic material". USA Patent US 5759564 A, 2 June 1998.

[82] T. J. Beveridge and W. S. Fyfe, "Metal fixation by bacterial cell walls," *Canadian Journal of Earth Sciences,* vol. 22, 1985.

[83] S. J. Rehm and J. G. Bartlett, "Challenges in the Management of Serious Infections," *Clinical Infectious Diseases - Oxford Journals,* vol. 42, no. S2, 2006.

[84] Y. Shai, "Mode of action of membrane active antimicrobial peptides," *Biopolymers,* vol. 66, no. 4, 2002.

[85] D. D. Bannerman, M. J. Paape, J. Lee, X. Zhao, J. C. Hope and P. Rainard, "Escherichia coli and Staphylococcus aureus Elicit Differential Innate Immune Responses following Intramammary Infection," *Clinical and Vaccine Immunology,* vol. 11, no. 3, 2004.

[86] A. V. Lombardi, K. R. Berend, J. B. Adams and J. M. Karnes, "Articulating Antibiotic Spacers: The Standard of Care for an Infected Total Knee Arthroplasty," *Orthopedics*, vol. 30 , no. 9, 2007.

[87] MetalPrices.com, [Online]. Available: www.metalprices.com. [Accessed 30 April 2013].

APPENDICES

APPENDIX A: Observations from Experiments on *S. aureus*

1st Replication

Electrode Configuration Ag-Ag							
l, ESD (mm)		Sample 1			Sample 2		
		L (mm)	W (mm)	Area (mm^2)	L (mm)	W (mm)	Area (mm^2)
l = 10	ESD = 10	26.00	10.66	277.16	24.00	14.00	336.00
	ESD = 20	25.00	10.66	266.50	23.50	13.66	321.01
	ESD = 40	27.00	11.60	313.20	23.50	13.66	321.01
l = 20	ESD = 10	25.00	10.66	266.50	23.50	13.00	305.50
	ESD = 20	27.00	10.66	287.82	23.50	12.66	297.51
	ESD = 40	27.00	12.33	332.91	24.00	13.66	327.84

Electrode Configuration Ag-Ti							
l, ESD (mm)		Sample 1			Sample 2		
		L (mm)	W (mm)	Area (mm^2)	L (mm)	W (mm)	Area (mm^2)
l = 10	ESD = 10	22.50	9.00	202.50	25.00	10.33	258.25
	ESD = 20	23.00	8.00	184.00	0.00	0.00	0.00
	ESD = 40	24.00	9.00	216.00	25.00	10.00	250.00
l = 20	ESD = 10	25.00	9.50	237.50	25.00	8.83	220.75
	ESD = 20	22.00	7.00	154.00	21.00	6.66	139.86
	ESD = 40	20.00	8.66	173.20	0.00	0.00	0.00

Electrode Configuration Ag-SS							
l, ESD (mm)		Sample 1			Sample 2		
		L (mm)	W (mm)	Area (mm^2)	L (mm)	W (mm)	Area (mm^2)
l = 10	ESD = 10	24.00	10.00	240.00	22.00	9.33	205.26
	ESD = 20	25.00	10.66	266.50	21.00	7.00	147.00
	ESD = 40	24.00	9.33	223.92	25.00	11.00	275.00
l = 20	ESD = 10	19.00	6.00	114.00	24.00	10.33	207.00
	ESD = 20	0.00	0.00	0.00	24.00	9.66	231.84
	ESD = 40	24.00	10.66	255.84	25.00	11.00	275.00

2nd Replication

Electrode Configuration Ag-Ag							
l, ESD (mm)		Sample 1			Sample 2		
		L (mm)	W (mm)	Area (mm^2)	L (mm)	W (mm)	Area (mm^2)
l = 10	ESD = 10	0.00	0.00	0.00	21.50	9.00	193.50
	ESD = 20	24.00	9.33	223.92	21.00	7.33	153.93
	ESD = 40	22.50	10.66	239.85	25.00	11.66	291.50
l = 20	ESD = 10	24.00	9.66	231.84	23.00	9.33	214.59
	ESD = 20	22.00	8.00	176.00	21.00	7.66	160.86
	ESD = 40	20.00	7.66	153.20	20.00	9.00	180.00

Electrode Configuration Ag-Ti							
l, ESD (mm)		Sample 1			Sample 2		
		L (mm)	W (mm)	Area (mm^2)	L (mm)	W (mm)	Area (mm^2)
l = 10	ESD = 10	21.00	7.66	160.86	22.00	9.00	198.00
	ESD = 20	24.50	9.66	236.67	20.00	7.50	150.00
	ESD = 40	21.00	10.16	213.36	0.00	0.00	0.00
l = 20	ESD = 10	23.00	9.50	218.50	0.00	0.00	0.00
	ESD = 20	22.00	8.66	190.52	23.00	8.33	191.59
	ESD = 40	22.00	8.50	187.00	21.00	9.00	189.00

Electrode Configuration Ag-SS							
l, ESD (mm)		Sample 1			Sample 2		
		L (mm)	W (mm)	Area (mm^2)	L (mm)	W (mm)	Area (mm^2)
l = 10	ESD = 10	20.00	6.83	136.60	20.00	6.83	136.60
	ESD = 20	20.00	6.83	136.60	18.00	7.16	128.88
	ESD = 40	0.00	0.00	0.00	17.00	9.00	153.00
l = 20	ESD = 10	25.00	10.33	258.25	21.50	8.16	175.44
	ESD = 20	20.00	8.16	163.20	17.00	6.66	113.22
	ESD = 40	15.00	6.83	102.45	20.00	8.66	173.20

3rd Replication

Electrode Configuration Ag-Ag							
l, ESD (mm)		Sample 1			Sample 2		
		L (mm)	W (mm)	Area (mm^2)	L (mm)	W (mm)	Area (mm^2)
l = 10	ESD = 10	20.00	6.00	120.00	22.00	9.50	209.00
	ESD = 20	21.00	8.16	171.36	0.00	0.00	0.00
	ESD = 40	20.00	8.33	166.60	24.00	10.33	247.92
l = 20	ESD = 10	21.00	8.00	168.00	20.00	7.50	150.00
	ESD = 20	22.00	9.00	198.00	20.00	7.16	143.20
	ESD = 40	20.00	8.16	163.20	21.00	8.83	185.43

Electrode Configuration Ag-Ti							
l, ESD (mm)		Sample 1			Sample 2		
		L (mm)	W (mm)	Area (mm^2)	L (mm)	W (mm)	Area (mm^2)
l = 10	ESD = 10	20.00	7.83	156.60	22.00	8.83	194.26
	ESD = 20	22.00	9.16	201.52	22.00	8.66	190.52
	ESD = 40	22.50	9.33	209.93	23.50	9.00	211.50
l = 20	ESD = 10	21.00	7.50	157.50	23.00	9.00	207.00
	ESD = 20	21.00	7.83	164.43	20.00	7.16	143.20
	ESD = 40	22.00	7.83	172.26	0.00	0.00	0.00

Electrode Configuration Ag-SS							
l, ESD (mm)		Sample 1			Sample 2		
		L (mm)	W (mm)	Area (mm^2)	L (mm)	W (mm)	Area (mm^2)
l = 10	ESD = 10	24.00	10.50	252.00	23.50	9.00	211.50
	ESD = 20	27.00	10.66	287.82	23.00	10.00	230.00
	ESD = 40	17.50	7.83	137.03	28.00	12.00	336.00
l = 20	ESD = 10	25.00	10.66	266.50	30.00	8.83	264.90
	ESD = 20	23.00	9.66	222.18	23.00	9.33	214.59
	ESD = 40	24.00	11.66	279.84	23.00	12.33	283.59

APPENDIX B: Observations from Experiments on *E. coli*

1st Replication						
Electrode Configuration	Sample 1			Sample 2		
	L (mm)	W (mm)	Area (mm^2)	L (mm)	W (mm)	Area (mm^2)
Ag-Ag	21.00	7.00	147.00	20.00	7.66	153.20
Ag-Ti	20.00	6.66	133.20	22.00	7.50	165.00
Ag-SS	0.00	0.00	0.00	24.00	9.33	223.92

2nd Replication						
Electrode Configuration	Sample 1			Sample 2		
	L (mm)	W (mm)	Area (mm^2)	L (mm)	W (mm)	Area (mm^2)
Ag-Ag	26.00	9.33	242.58	0.00	0.00	0.00
Ag-Ti	22.50	9.66	217.35	25.00	9.50	237.50
Ag-SS	21.50	8.16	175.44	0.00	0.00	0.00

3rd Replication						
Electrode Configuration	Sample 1			Sample 2		
	L (mm)	W (mm)	Area (mm^2)	L (mm)	W (mm)	Area (mm^2)
Ag-Ag	20.00	6.66	133.20	20.00	7.33	146.60
Ag-Ti	18.00	6.66	119.88	23.00	8.83	203.09
Ag-SS	21.00	6.33	132.93	21.00	6.66	139.86

APPENDIX C: Additional Experimental Results

Anode and Cathode Length = 25mm

1st Replication						
Electrode Configuration	Anode Inhibition Zone			Cathode Inhibition Zone		
	L (mm)	W (mm)	Area (mm^2)	L (mm)	W (mm)	Area (mm^2)
Ag-Ag	28.00	13.00	364.00	27.00	13.33	359.91
Ag-Ti	30.00	13.33	399.90	23.00	8.83	203.09
Ag-SS	28.00	14.33	401.24	21.00	6.66	139.86

2nd Replication						
Electrode Configuration	Anode Inhibition Zone			Cathode Inhibition Zone		
	L (mm)	W (mm)	Area (mm^2)	L (mm)	W (mm)	Area (mm^2)
Ag-Ag	28.00	14.00	392.00	27.50	13.66	375.65
Ag-Ti	29.00	14.66	425.14	0.00	0.00	0.00
Ag-SS	0.00	0.00	0.00	-	-	-

3rd Replication						
Electrode Configuration	Anode Inhibition Zone			Cathode Inhibition Zone		
	L (mm)	W (mm)	Area (mm^2)	L (mm)	W (mm)	Area (mm^2)
Ag-Ag	27.00	12.00	324.00	26.00	13.00	338.00
Ag-Ti	28.50	13.33	379.91	0.00	0.00	0.00
Ag-SS	28.00	13.00	364.00	-	-	-

Note: All values in the above tables with a "0.00" indicate no inhibition zone. Values marked "-" had inhibition zones which were not clearly visible and hence could not be measured.

APPENDIX D: Images of Experiments on *S. aureus*

1st Replication

ESD = 10 mm ESD = 20 mm ESD = 40 mm

Ag-Ag Sample 1

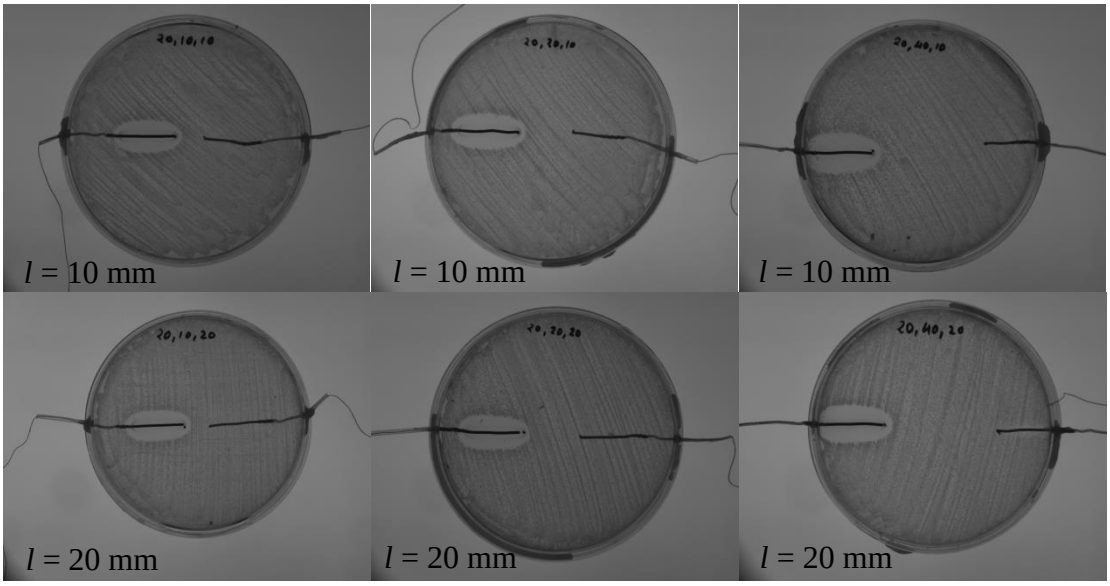

Ag-Ag Sample 2

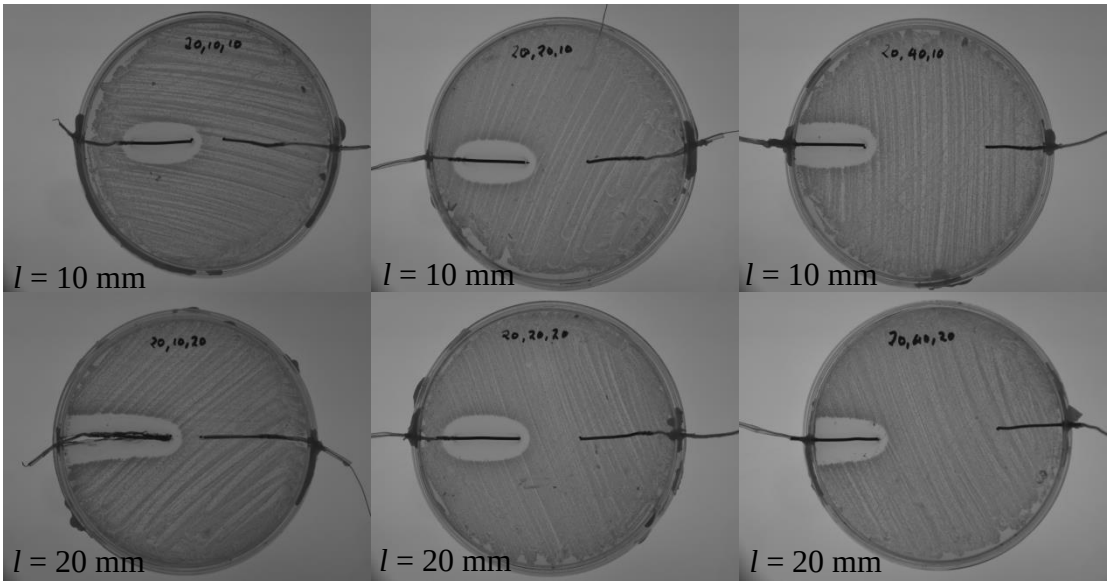

1st Replication

ESD = 10 mm ESD = 20 mm ESD = 40 mm

Ag-Ti Sample 1

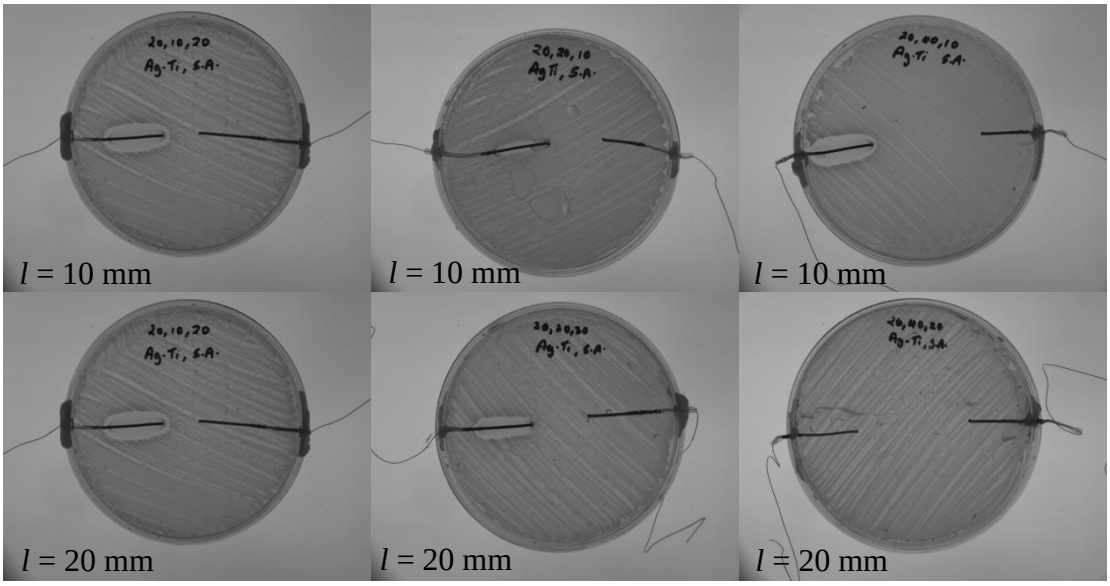

Ag-Ti Sample 2

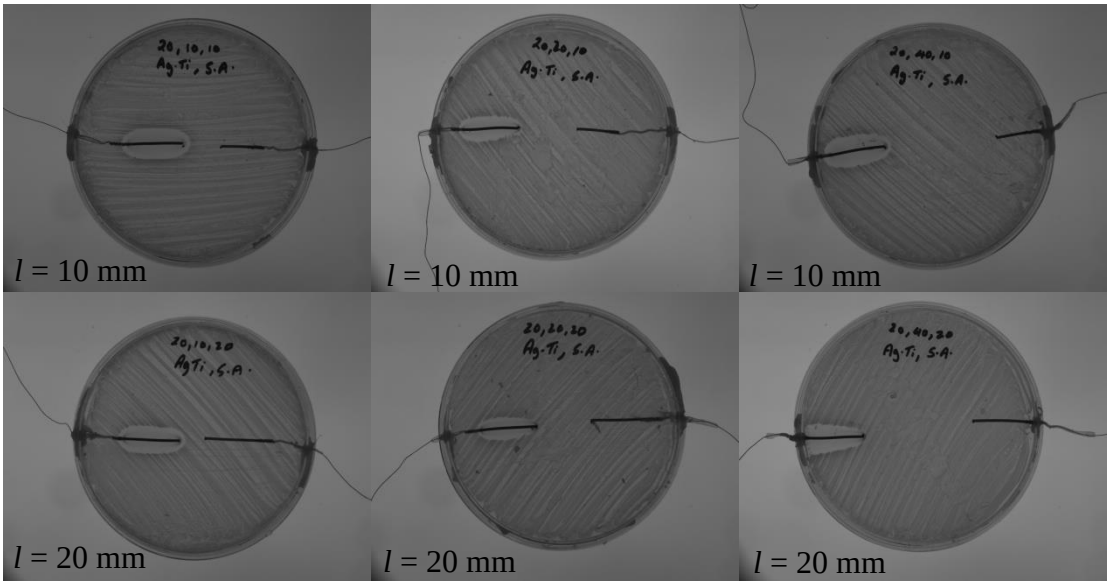

1st Replication

ESD = 10 mm ESD = 20 mm ESD = 40 mm

Ag-SS Sample 1

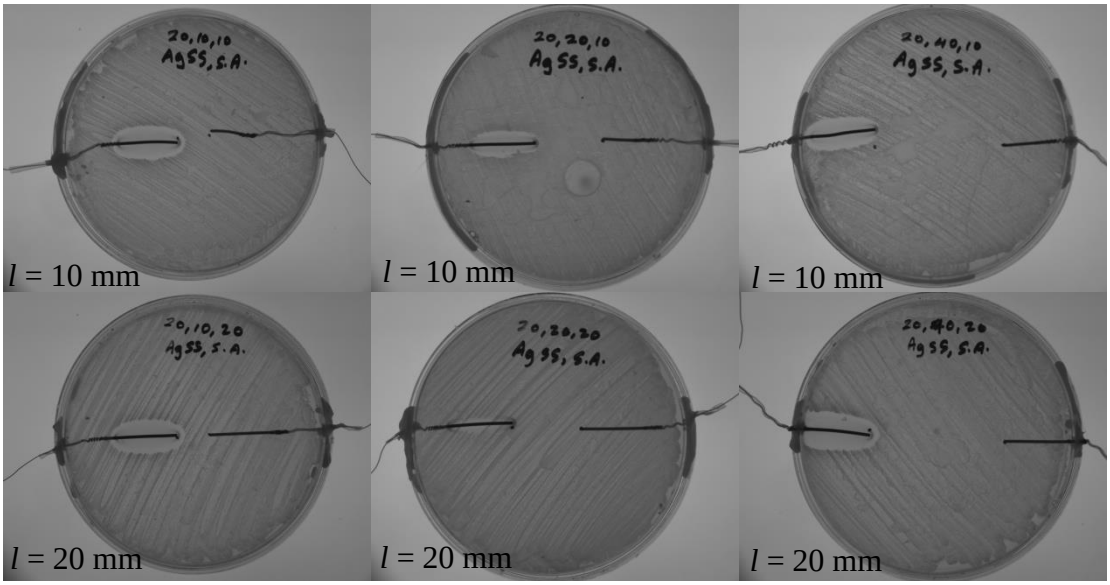

Ag-SS Sample 2

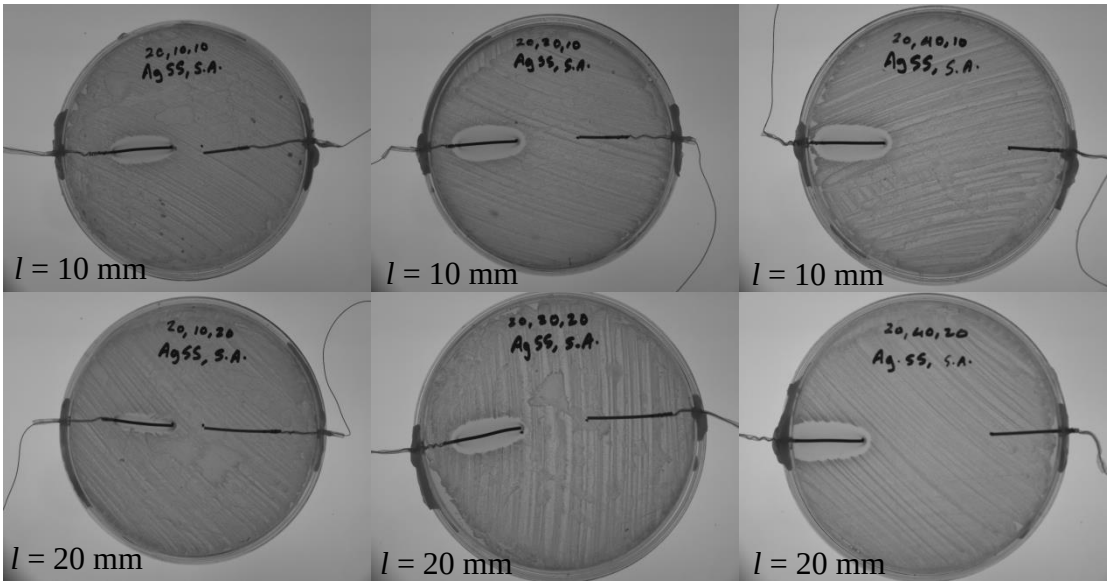

2nd Replication

ESD = 10 mm ESD = 20 mm ESD = 40 mm

Ag-Ag Sample 1

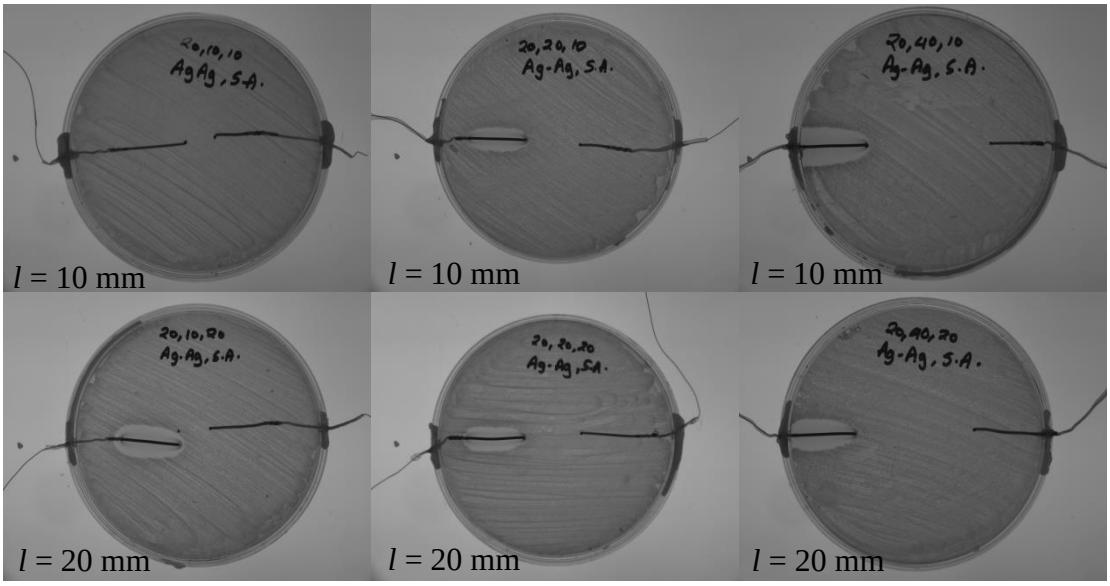

l = 10 mm *l* = 10 mm *l* = 10 mm

l = 20 mm *l* = 20 mm *l* = 20 mm

Ag-Ag Sample 2

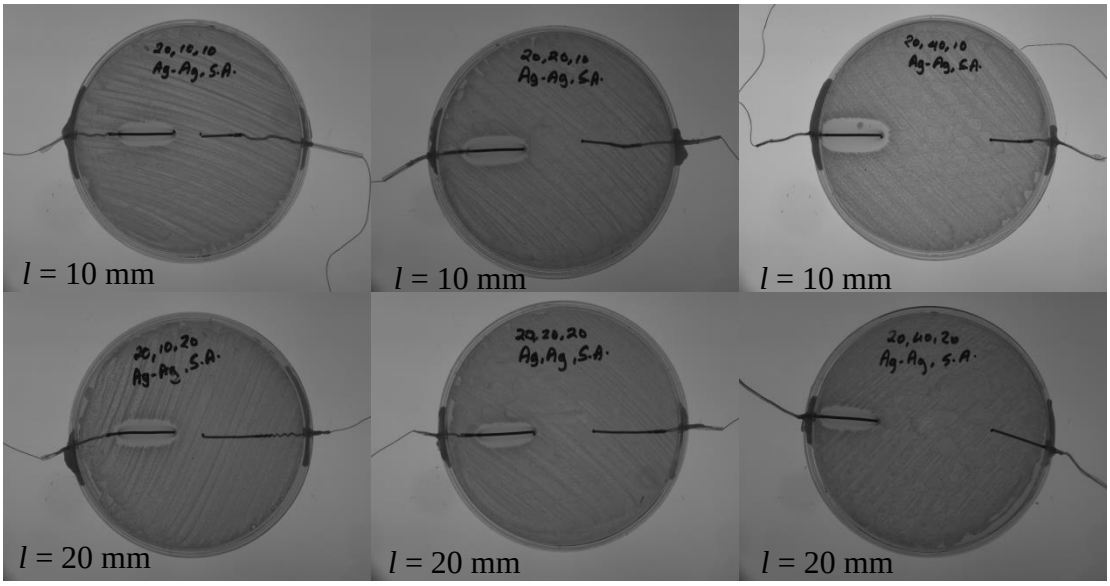

l = 10 mm *l* = 10 mm *l* = 10 mm

l = 20 mm *l* = 20 mm *l* = 20 mm

2nd Replication

ESD = 10 mm ESD = 20 mm ESD = 40 mm

Ag-Ti Sample 1

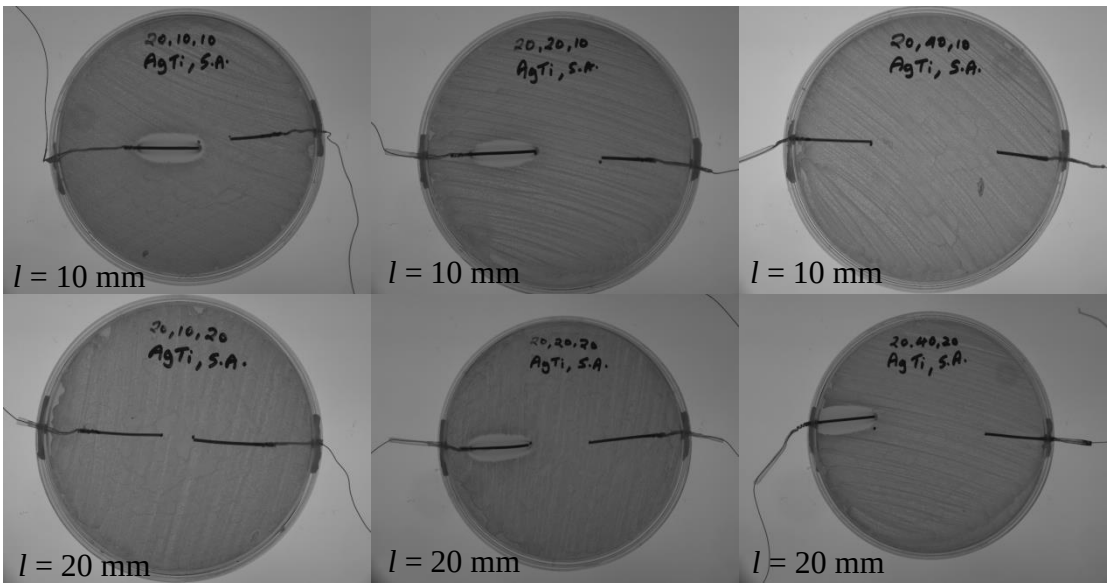

Ag-Ti Sample 2

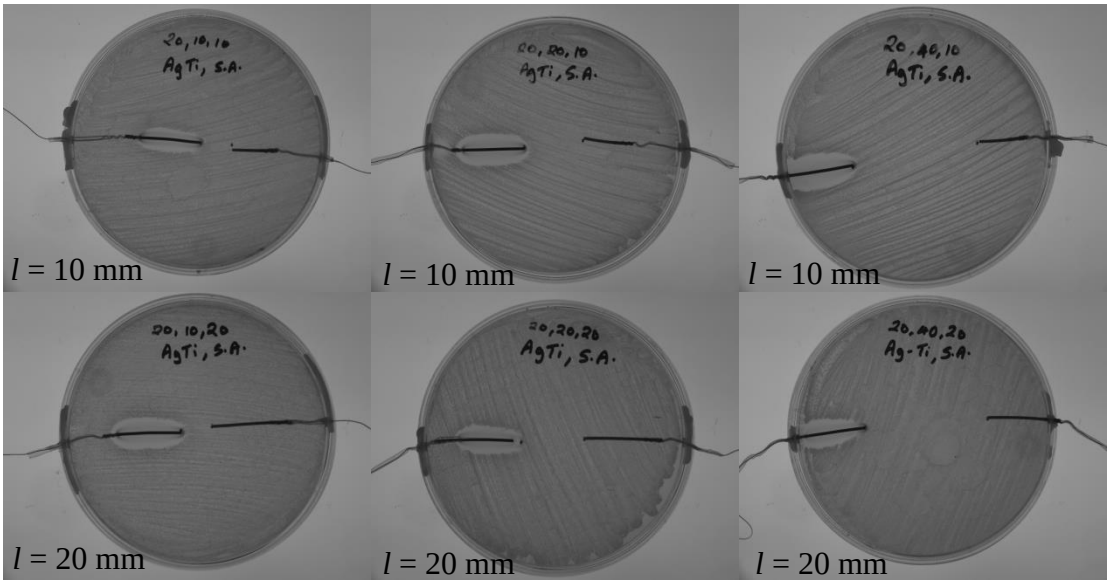

2nd Replication

ESD = 10 mm ESD = 20 mm ESD = 40 mm

Ag-SS Sample 1

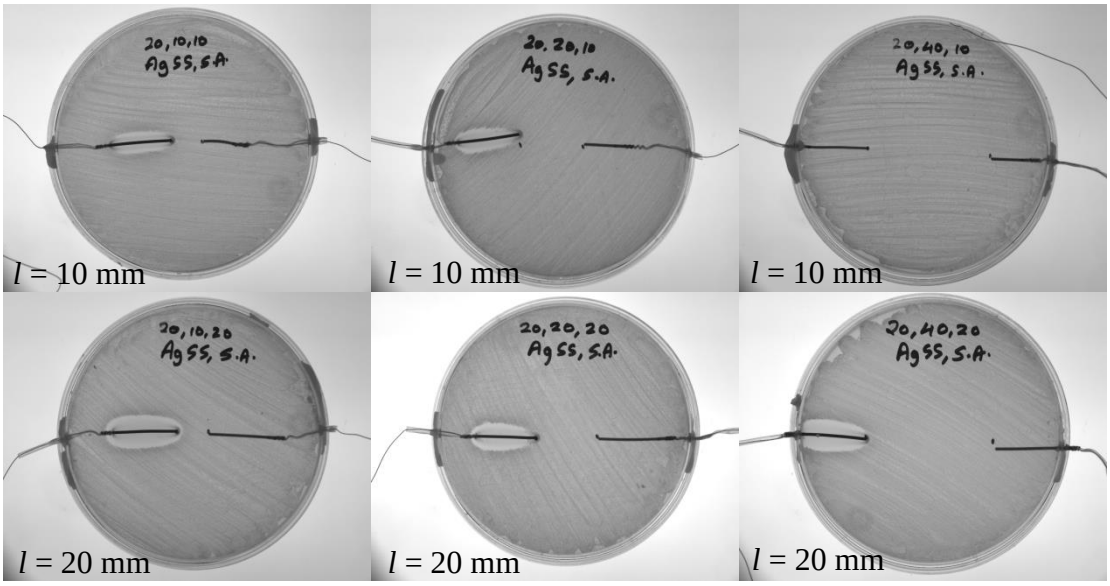

l = 10 mm *l* = 10 mm *l* = 10 mm

l = 20 mm *l* = 20 mm *l* = 20 mm

Ag-SS Sample 2

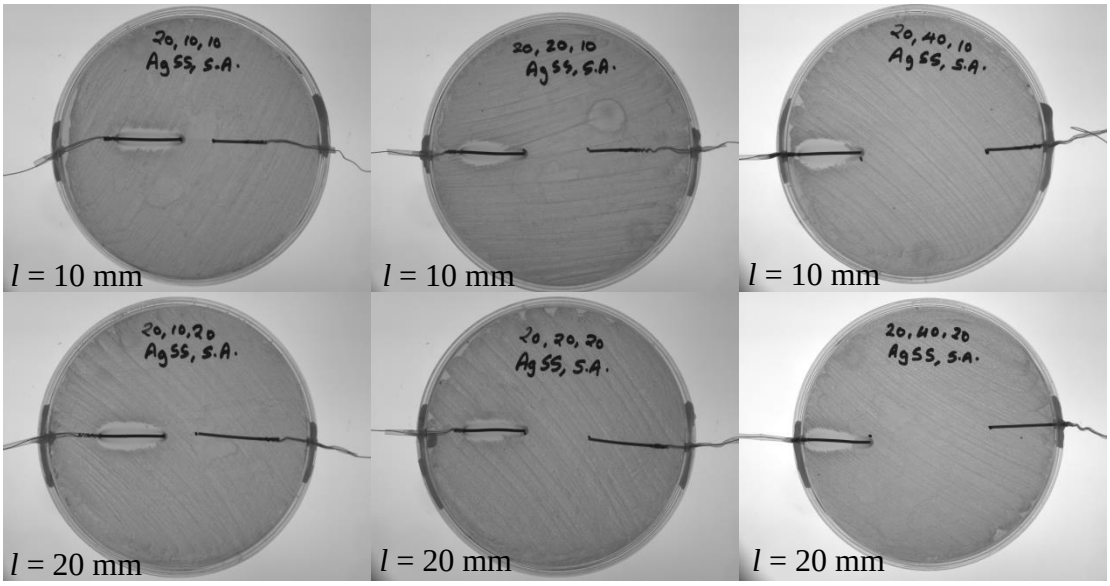

l = 10 mm *l* = 10 mm *l* = 10 mm

l = 20 mm *l* = 20 mm *l* = 20 mm

3rd Replication

ESD = 10 mm ESD = 20 mm ESD = 40 mm

Ag-Ag Sample 1

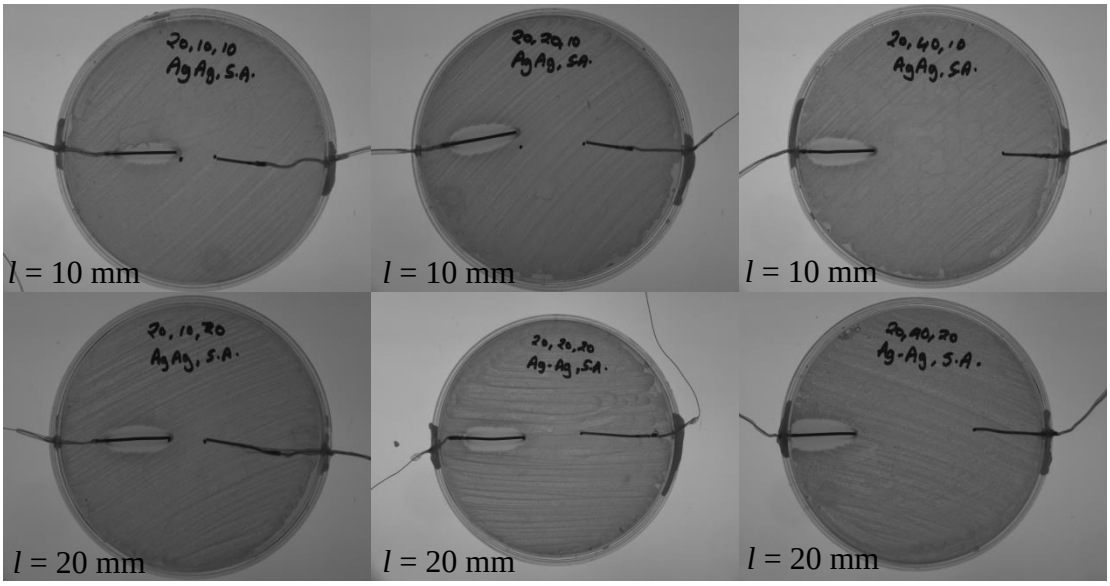

Ag-Ag Sample 2

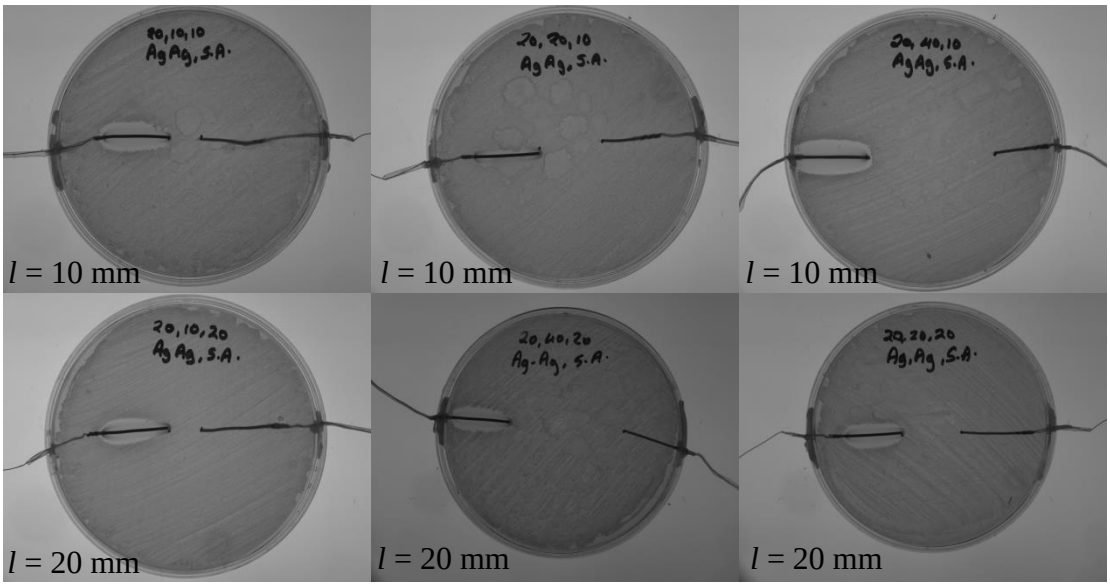

3rd Replication

ESD = 10 mm ESD = 20 mm ESD = 40 mm

Ag-SS Sample 1

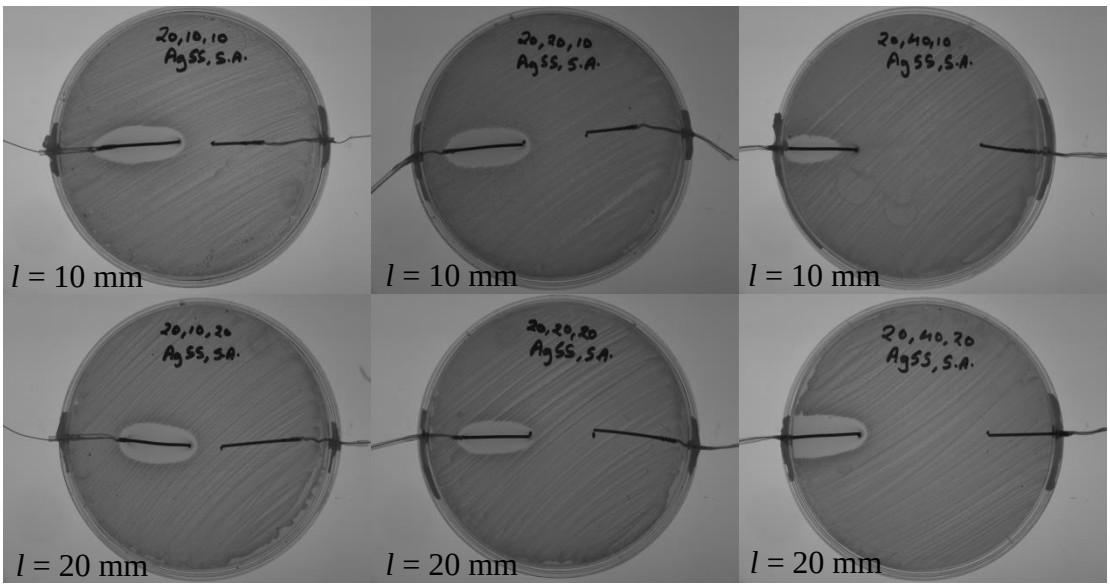

Ag-SS Sample 2

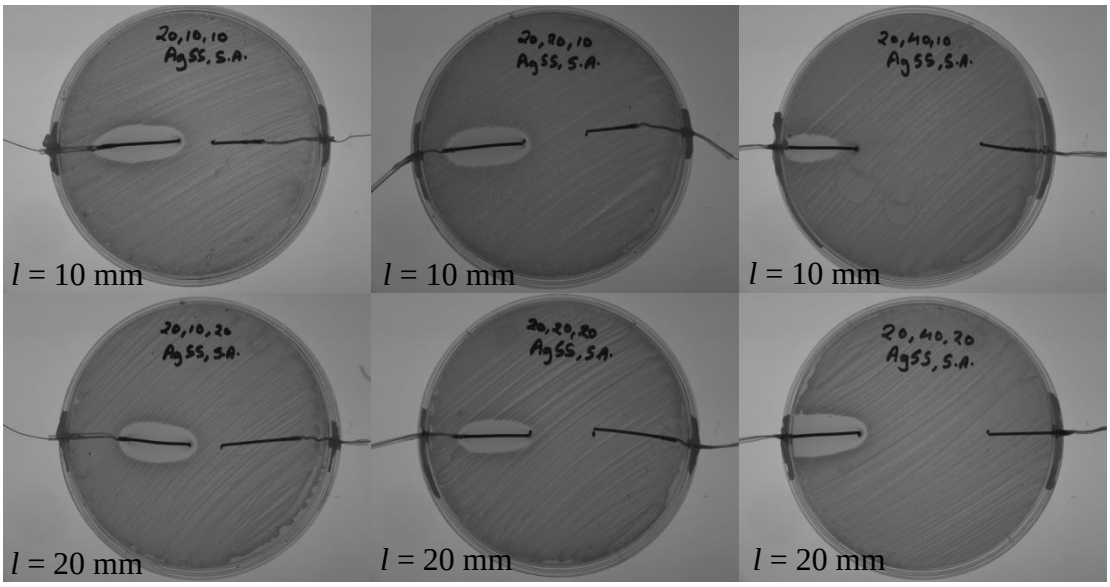

Note: The images of Ag-Ti's 3rd Replication have not been included due to file corruption

APPENDIX E: Images of Experiments on *E. coli*

1st Replication

Ag-Ag	Ag-Ti	Ag-SS
ESD = 20 mm	ESD = 20 mm	ESD = 20 mm

Sample 1

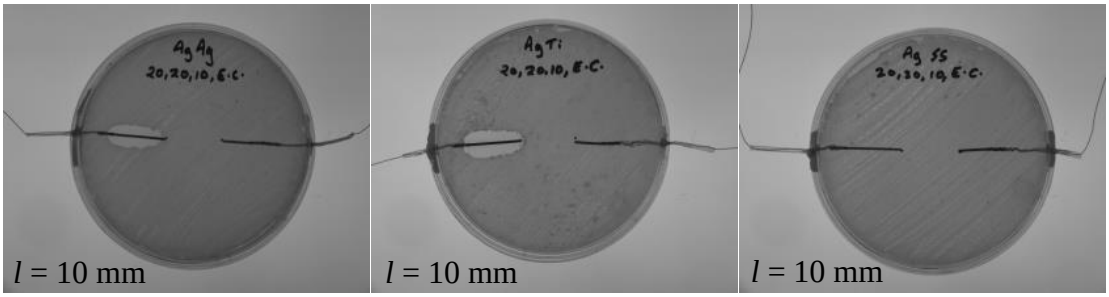

l = 10 mm | *l* = 10 mm | *l* = 10 mm

Sample 2

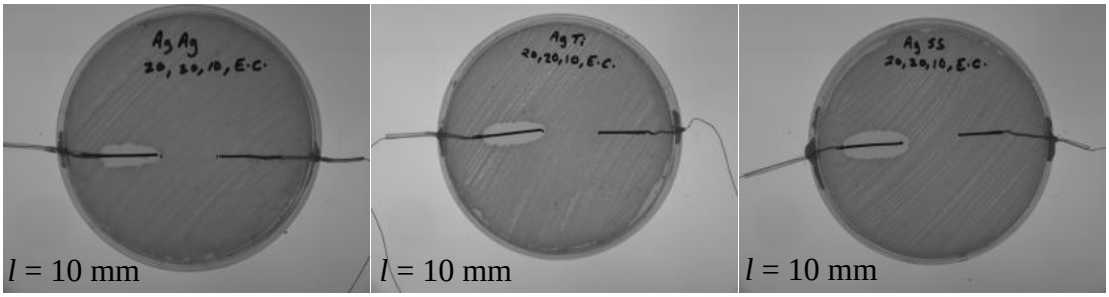

l = 10 mm | *l* = 10 mm | *l* = 10 mm

2nd Replication

Ag-Ag	Ag-Ti	Ag-SS
ESD = 20 mm	ESD = 20 mm	ESD = 20 mm

Sample 1

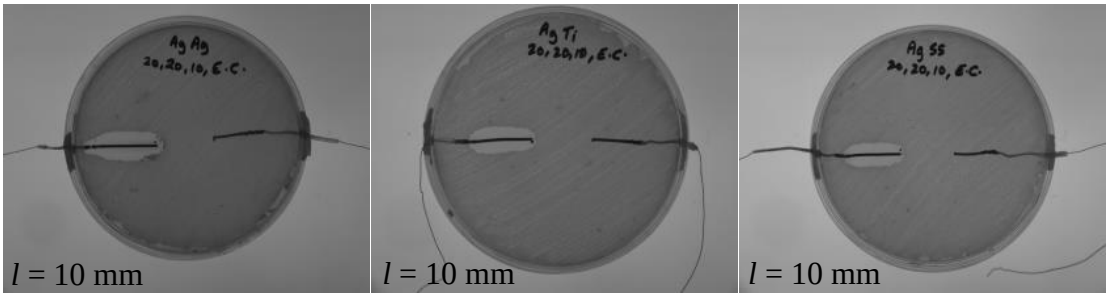

l = 10 mm *l* = 10 mm *l* = 10 mm

Sample 2

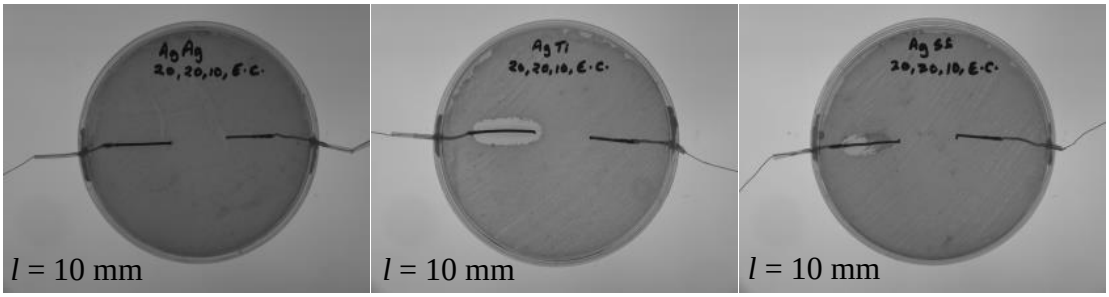

l = 10 mm *l* = 10 mm *l* = 10 mm

3rd Replication

Ag-Ag	Ag-Ti	Ag-SS
ESD = 20 mm	ESD = 20 mm	ESD = 20 mm

Sample 1

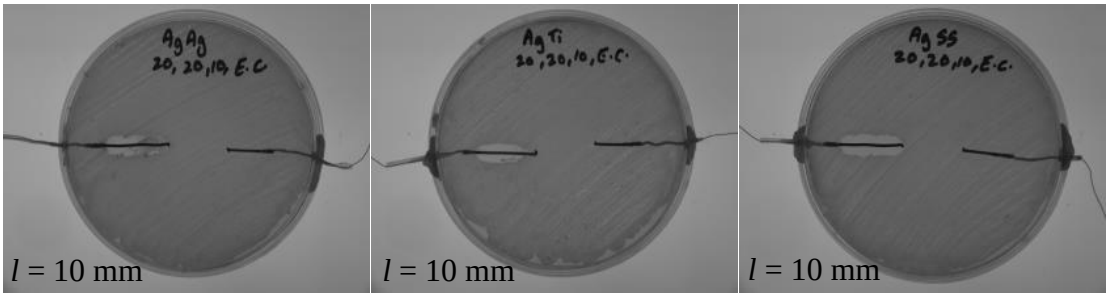

l = 10 mm | *l* = 10 mm | *l* = 10 mm

Sample 2

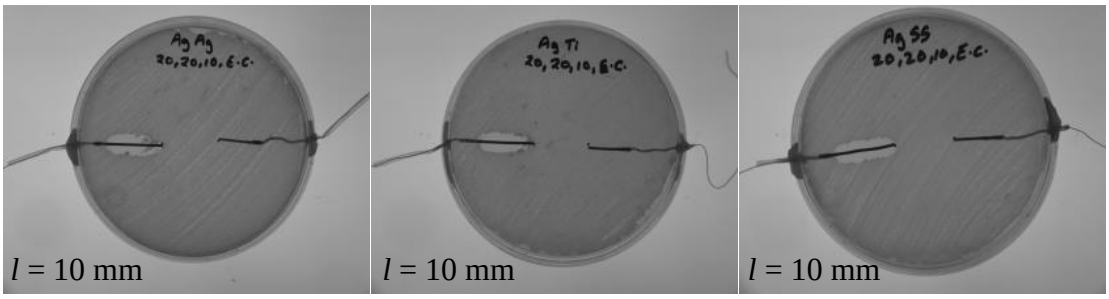

l = 10 mm | *l* = 10 mm | *l* = 10 mm